EUROPEAN ORGANIZATION FOR NUCLEAR RESEARCH

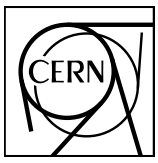

CERN-EP-2023-196
30 August 2023

Measurements of long-range two-particle correlation over a wide pseudorapidity range in p–Pb collisions at $\sqrt{s_{\mathrm{NN}}}$ = 5.02 TeV

ALICE Collaboration*

Abstract

Correlations in azimuthal angle extending over a long range in pseudorapidity between particles, usually called the "ridge" phenomenon, were discovered in heavy-ion collisions, and later found in pp and p–Pb collisions. In large systems, they are thought to arise from the expansion (collective flow) of the produced particles. Extending these measurements over a wider range in pseudorapidity and final-state particle multiplicity is important to understand better the origin of these long-range correlations in small collision systems. In this Letter, measurements of the long-range correlations in p–Pb collisions at $\sqrt{s_{\mathrm{NN}}} = 5.02$ TeV are extended to a pseudorapidity gap of $\Delta\eta{\sim}8$ between particles using the ALICE forward multiplicity detectors. After suppressing non-flow correlations, e.g., from jet and resonance decays, the ridge structure is observed to persist up to a very large gap of $\Delta\eta{\sim}8$ for the first time in p–Pb collisions. This shows that the collective flow-like correlations extend over an extensive pseudorapidity range also in small collision systems such as p–Pb collisions. The pseudorapidity dependence of the second-order anisotropic flow coefficient, $v_2(\eta)$, is extracted from the long-range correlations. The $v_2(\eta)$ results are presented for a wide pseudorapidity range of $-3.1 < \eta < 4.8$ in various centrality classes in p–Pb collisions. To gain a comprehensive understanding of the source of anisotropic flow in small collision systems, the $v_2(\eta)$ measurements are compared with hydrodynamic and transport model calculations. The comparison suggests that the final-state interactions play a dominant role in developing the anisotropic flow in small collision systems.

*See Appendix B for the list of collaboration members

1 Introduction

High-energy heavy-ion collisions can produce a deconfined state of quarks and gluons, the so-called quark–gluon plasma (QGP). Measurements of azimuthal anisotropic flow, for example, via long-range two-particle correlations, are sensitive to key properties of the QGP [1]. The two-particle correlations between an associated particle and a trigger particle are commonly measured as a function of the differences in pseudorapidity ($\Delta\eta = \eta_{\rm trig} - \eta_{\rm asso}$) and azimuthal angle ($\Delta\varphi = \varphi_{\rm trig} - \varphi_{\rm asso}$). Striking correlations over a long range in $\Delta\eta$ on the near side ($\Delta\varphi \sim 0$), the so-called "ridge", have been observed in heavy-ion collisions [2–11], where they are well understood as a consequence of strong, final-state interactions in the dense system created in heavy-ion collisions and the resulting fluid-like collective expansion of the matter created. The correlation function, associate yield as a function of differences in pseudorapidity and azimuthal angle, projected onto the $\Delta\varphi$ direction, can be expressed in terms of a Fourier series,

$$\frac{{\rm d}N_{\rm pair}}{{\rm d}\Delta\varphi} \propto 1 + \sum_{n=1}^{\infty} 2v_n^2 \cos\left(n\Delta\varphi\right), \tag{1}$$

where v_n is the Fourier coefficient of n-th flow harmonics. The v_n coefficients emerge due to the anisotropic hydrodynamic expansion of the medium and fluctuate along with the collision geometry in heavy-ion collisions. The v_n coefficients and their multiplicity and transeverse-momentum ($p_{\rm T}$) dependence are well described by relativistic hydrodynamic models at midrapidity [12, 13]. The pseudorapidity dependence of v_n coefficients is sensitive to a temperature dependence of the shear viscosity to entropy density ratio η/s of the QGP [14–16]. It has been measured over a large pseudorapidity region ($|\eta| < 5$) in Au–Au and Pb–Pb collisions at RHIC [17] and the LHC [18]. In small collision systems, such as pp and p–Pb collisions, a "ridge" structure was also observed similar to heavy-ion collisions [19–31]. The $p_{\rm T}$ dependence of v_n coefficients in small collision systems, which shows a characteristic mass dependence at low $p_{\rm T}$, is found to be similar to heavy-ion collisions [27, 29, 31, 32]. Both hydrodynamic (macroscopic) and kinetic transport (microscopic) models can describe collective-flow observables fairly well in small systems as well as in heavy-ion collisions [33–38]. However, the underlying physics of the observed anisotropic flow in small collision systems is still under debate. One possible scenario predicts that both contributions from a momentum anisotropy arising in the initial state as well as final interactions are essential in small collision systems [39–41]. Furthermore, the relative contributions of soft collective processes, concentrated in the dense "core" and modeled with hydrodynamics, and of hard processes such as hard scattering and jet fragmentation (described as a pp-like "corona") are also not well understood. The charged-particle pseudorapidity distribution is asymmetric in p–Pb collisions [42]: the multiplicity is larger in the Pb-going direction compared to the p-going direction. Since the mean free path depends on the charged-particle multiplicity, the pseudorapidity dependence of v_2 reflects the underlying dynamical evolution in p–Pb collisions and is a direct indicator of how local particle densities modulate the collective flow. CMS results on $v_2(\eta)$ in p–Pb collisions at the LHC [43, 44] show a significant pseudorapidity dependence, beyond what would be expected from the pseudorapidity dependence of the mean $p_{\rm T}$. However, the acceptance is limited to midrapidity $|\eta| < 2$. Various small asymmetric collision systems were used to extract $v_2(\eta)$ at RHIC by means of the event plane method. The measurements were carried out within the pseudorapidity range of $|\eta| < 3$ [45, 46]. A hydrodynamic model [47] describes the result of $v_2(\eta)$ qualitatively except for the pseudorapidity regions ($-3 < \eta < -2$) in p–Au collisions, where non-flow effects appear to be significant because the rapidity gap from the detector that determines the event plane is small.

In this Letter, the measurements of long-range two-particle correlations and $v_2(\eta)$ in p–Pb collisions at $\sqrt{s_{\rm NN}} = 5.02$ TeV with the ALICE detector at the LHC are presented. These measurements utilize the Forward Multiplicity Detector (FMD) to extract $v_2(\eta)$ over the unprecedented range of about 8 units of pseudorapidity ($-3.1 < \eta < 4.8$). The results are compared with a hydrodynamic-model calculation and the AMPT transport model.

2 Experimental setup

A comprehensive description of the ALICE detector can be found in Refs. [48, 49]. The main detectors used in this analysis are the Forward Multiplicity Detector (FMD), the Inner Tracking System (ITS), and the Time Projection Chamber (TPC). The FMD is a silicon strip detector that measures charged particles with a fine granularity of $\Delta\varphi = \pi/20$ and $\Delta\eta = 0.05$. The FMD comprises three sub-detectors: FMD1, FMD2, and FMD3. The combined acceptance of FMD1 and FMD2 is $1.7 < \eta < 5.1$. The pseudorapidity coverage of FMD3 is $-3.4 < \eta < -1.7$. FMD1 and FMD3 consist of an inner and an outer ring, and FMD2 consists of only one ring, all placed around the beam pipe. The inner and outer rings are divided into 20 and 40 sectors in the azimuthal direction, respectively, and each ring is composed of hexagonal silicon sensors. Each inner and outer ring is segmented into 512 and 256 strips in the radial direction, respectively. Charged-particle tracking at midrapidity is provided using the TPC and ITS, both covering the full azimuthal angle and $|\eta| < 0.8$. They are placed inside the L3 solenoid magnet, which provides a magnetic field of $B = 0.5$ T along the beam direction. The vertex detector, ITS, consists of six layers of silicon detectors; two layers each are equipped with the Silicon Pixel Detector (SPD), the Silicon Drift Detector (SDD), and the Silicon Strip Detector (SSD). The TPC provides track reconstruction using up to 159 space points along a charged-particle trajectory and particle identification via the measurement of specific energy loss $\mathrm{d}E/\mathrm{d}x$. The V0 is used for event triggering and centrality determination. It is composed of two arrays of 32 scintillator tiles each and covers $-3.7 < \eta < -1.7$ (V0C) and $2.8 < \eta < 5.1$ (V0A). In addition, two neutron Zero Degree Calorimeters (ZDCs) located at 112.5 m (ZNA) and -112.5 m (ZNC) from the interaction point along the beam direction are used for the event selection.

3 Data analysis

3.1 Event and Track selection

This analysis uses ALICE data taken for p–Pb collisions at a centre-of-mass energy per nucleon pair of $\sqrt{s_{\mathrm{NN}}} = 5.02$ TeV provided by the LHC in 2016, corresponding to a proton beam energy of 4 TeV and a lead beam energy of 1.58 TeV per nucleon. Due to the asymmetric collision system, the nucleon–nucleon centre-of-mass system was shifted by 0.465 rapidity units in the proton beam direction with respect to the ALICE laboratory system. In this Letter, η denotes the pseudorapidity in the laboratory system, and the positive pseudorapidity points in the Pb-going direction.

This analysis uses 5×10^8 events acquired using a minimum bias trigger. The minimum bias trigger requires the in-time coincidence of signals from V0A and V0C. The first step of the event selection is performed on the amplitude and timing in the V0 and ZDC as described in Ref. [50]. The efficiency of the event selection is 99.2% for non-single-diffractive collisions. The primary vertex position is determined with reconstructed tracks in the TPC and ITS by using an analytic χ^2 minimization method as described in Ref. [51]. The primary vertex in the beam axis is required to be within 10 cm of the nominal interaction point along the beam line. In addition, pile-up events from beam-induced background are rejected by using correlations between the FMD and V0 multiplicities.

Charged-particle tracks are reconstructed in the ITS and TPC within $|\eta| < 0.8$ for $p_{\mathrm{T}} > 0.2$ GeV/c as follows. First, the tracks are selected on the number of space points and the quality of the track fit in the TPC. In addition, the tracks are required to have a distance of closest approach (DCA) to the reconstructed primary vertices less than 2 cm in the beam-axis direction. The DCA in the transverse direction is required to be less than 7 σ_{DCA}, where σ_{DCA} is a p_{T}-dependent transverse impact parameter resolution. The efficiency of the charged-particle track selection is estimated with a Monte Carlo (MC) simulation using the DPMJET event generator [52] and GEANT3 [53] to simulate particle transport through the detector. The efficiency is about 65% at p_{T} =0.2 GeV/c, increases to about 79% at p_{T} =0.8 GeV/c, and decreases to about 76% at p_{T} =3 GeV/c.

The selected events are divided into several centrality classes based on the V0A amplitude. Table 1 shows the event classes and corresponding average charged-particle pseudorapidity densities within $-3.25 < \eta < -2.5$, $|\eta| < 0.8$, $2 < \eta < 3.75$, and $3.75 < \eta < 5$. The multiplicities were measured by the innermost two layers of the ITS at midrapidity and the FMD at forward and backward rapidity [42].

Table 1: Average charged-particle pseudorapidity density for $p_{\mathrm{T}} > 0$ GeV/c in different pseudorapidity regions.

Centrality	$\langle \mathrm{d}N_{\mathrm{ch}}/\mathrm{d}\eta \rangle_{-3.25<\eta<-2.5}$	$\langle \mathrm{d}N_{\mathrm{ch}}/\mathrm{d}\eta \rangle_{\lvert\eta\rvert<0.8}$	$\langle \mathrm{d}N_{\mathrm{ch}}/\mathrm{d}\eta \rangle_{2<\eta<3.75}$	$\langle \mathrm{d}N_{\mathrm{ch}}/\mathrm{d}\eta \rangle_{3.75<\eta<5}$
0–5%	34 ± 2.2	45 ± 1.4	60 ± 3.8	52 ± 3.5
5–10%	29 ± 1.9	36 ± 1.1	46 ± 2.9	39 ± 2.6
10–20%	26 ± 1.6	31 ± 0.94	37 ± 2.4	31 ± 2.1
20–40%	21 ± 1.4	23 ± 0.72	27 ± 1.7	22 ± 1.5
40–60%	16 ± 1.0	16 ± 0.54	17 ± 1.1	14 ± 0.95
60–80%	11 ± 0.68	9.7 ± 0.33	9.9 ± 0.63	7.8 ± 0.52
80–100%	5.4 ± 0.34	4.2 ± 0.14	3.5 ± 0.22	2.7 ± 0.18

3.2 Two-particle correlation and extraction of $v_2(\eta)$

For a given event class, two-particle correlations between a trigger and associated particle are measured as a function of the pseudorapidity difference $\Delta\eta$ and the azimuthal angle difference $\Delta\varphi$. The associated yield to a trigger particle as a function of $\Delta\eta$ and $\Delta\varphi$ is defined as

$$\frac{1}{N_{\mathrm{trig}}} \frac{\mathrm{d}^2 N_{\mathrm{assoc}}}{\mathrm{d}\Delta\eta \mathrm{d}\Delta\varphi} = \frac{S(\Delta\eta, \Delta\varphi)}{B(\Delta\eta, \Delta\varphi)}, \tag{2}$$

where N_{trig} is the total number of trigger particles in the given event class, the signal function $S(\Delta\eta, \Delta\varphi) = \frac{1}{N_{\mathrm{trig}}} \frac{\mathrm{d}^2 N_{\mathrm{same}}}{\mathrm{d}\Delta\eta \mathrm{d}\Delta\varphi}$ is the associated yield per trigger particle in the same event, and the background function $B(\Delta\eta, \Delta\varphi) = \alpha \frac{\mathrm{d}^2 N_{\mathrm{mixed}}}{\mathrm{d}\Delta\eta \mathrm{d}\Delta\varphi}$ is the pair yield associated to a trigger particle when the associated particles are taken from other events which fall in the same event class. The α factor is chosen such that $B(\Delta\eta, \Delta\varphi)$ is unity at its maximum. By dividing $S(\Delta\eta, \Delta\varphi)$ by $B(\Delta\eta, \Delta\varphi)$, pair acceptance and single particle efficiency for both particles are corrected. To take into account the vertex position dependence of the above acceptance and efficiency, the correlation function is extracted in 2 cm wide intervals of the vertex position.

Figure 1 shows the correlation function in $\Delta\eta$ and $\Delta\varphi$ between trigger and associated particles in TPC ($|\eta| < 0.8$) – FMD1,2 ($2.9 < \eta < 3.1$) (left), TPC– FMD3 ($-3.1 < \eta < -2.9$) (center), and FMD1,2 ($4.6 < \eta < 4.8$) – FMD3 ($-3.1 < \eta < -2.9$) (right) in the 0–5% (top) and 60–100% (bottom) p–Pb collisions at $\sqrt{s_{\mathrm{NN}}}$ = 5.02 TeV, respectively. For all three combinations, a long-range correlation on the near side ($-\pi/2 < \Delta\varphi < \pi/2$), the so-called "ridge", is observed in the 0–5% event class, while no significant "ridge" is observed in 60–100%. The long-range correlation in the away side ($\pi/2 < \Delta\varphi < 3\pi/2$) mainly results from jets recoiling opposite to the trigger particle and is visible in all event classes. Since the pseudorapidity gap between the trigger and associated particles is large, the pronounced peak structure on the near side due to jets [28], which is centred on $\Delta\eta = 0$, is not present. In central p–Pb collisions at the LHC, the near-side "ridge" structure is observed to extend up to a pseudorapidity separation of $\Delta\eta \sim 8$, which is the largest range measured.

To estimate and subtract the non-flow effects due to recoil jets and resonance decays, the template fit procedure, which was introduced by the ATLAS collaboration, is employed [54, 55]. The correlation function $Y(\Delta\varphi)$ is assumed to be a superposition of a non-flow contribution, which is estimated by scaling the correlation function from peripheral events, and the flow contribution. The template fit function is defined as

$$Y(\Delta\varphi) = FY^{\mathrm{peri}}(\Delta\varphi) + G^{\mathrm{tmp}}\{1 + 2\sum_{n=2}^{3} V_{n,n}^{\mathrm{tmp}} \cos(n\Delta\varphi)\}, \tag{3}$$

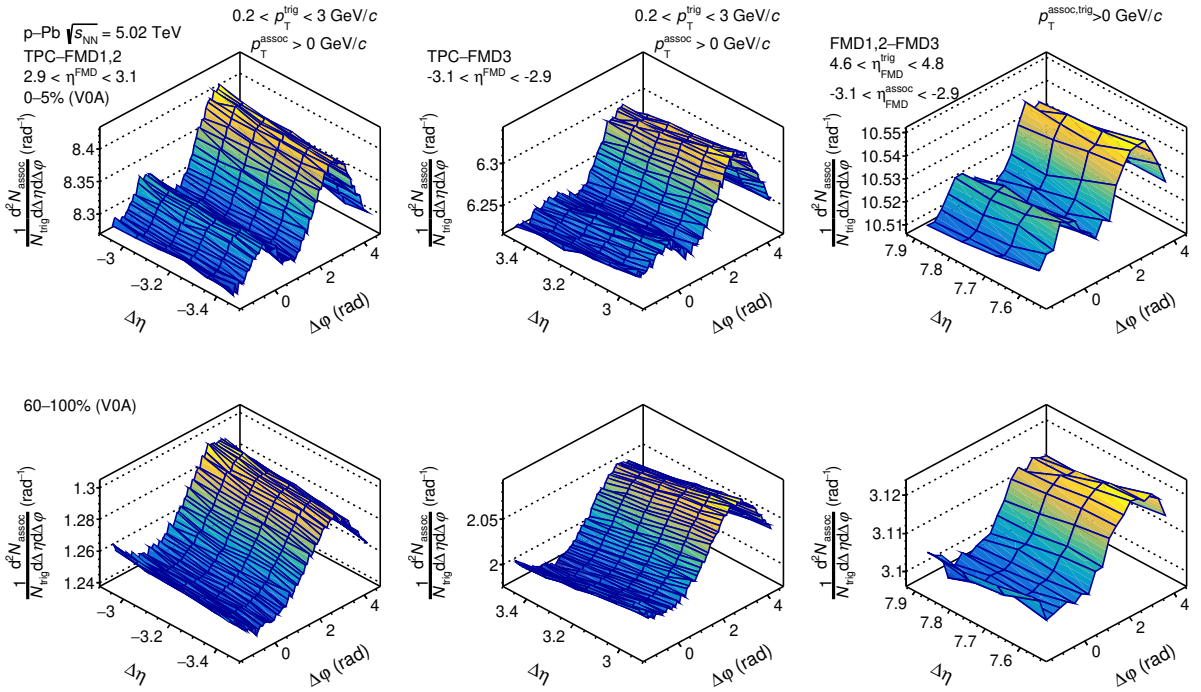

Figure 1: The associated yield per trigger as a function of $\Delta\eta$ and $\Delta\varphi$ as measured for TPC–FMD1,2 (left), TPC–FMD3 (central), and FMD1,2–FMD3 (right) correlations in the 0–5% (top) and 60–100% (bottom) p–Pb collisions.

where $F, G^{\rm tmp}$, and $V_{n,n}^{\rm tmp}$ are free parameters. $Y^{\rm peri}(\Delta\varphi)$ is the correlation function in peripheral events. $V_{n,n}^{\rm tmp}$ represents the n-th flow coefficient, and F and G are the scaling factors of the non-flow distribution on the away side and a flat, azimuth-independent baseline, respectively. This method assumes no flow components in the peripheral event used for the template and no away-side jet modifications between central and peripheral events.

Figure 2 shows the projection of the correlation functions, i.e., TPC–FMD1,2 (left), TPC–FMD3 (center), FMD1,2–FMD3 (right), onto the $\Delta\varphi$ axis in the 0–5% event class. These one-dimensional correlations are fitted by the template fit function using Eq. (3). The fit describes the data well with a χ^2/ndf of about 0.8–2.5 for all correlation functions corresponding to all η gap combinations. The flow-like part of the fit is dominated by the second harmonic for all three correlations. The modulation for the pair correlation is extracted for each harmonic in the template fit.

Assuming that the relative modulation of the two-particle correlation function is solely due to the modulation of the single-particle distribution, the modulation of the two-particle correlation measured in two different pseudorapidity ranges for particles a and b can be factorized as:

$$V_{n,n}(\eta_a,\eta_b) = v_n(\eta_a)v_n(\eta_b). \tag{4}$$

If this factorization holds, the flow component of a single particle at a certain pseudorapidity can be extracted from three dihadron correlations between different pseudorapidity regions given by

$$v_n(\eta_a) = \sqrt{\frac{V_{n,n}(\eta_a,\eta_b)V_{n,n}(\eta_a,\eta_c)}{V_{n,n}(\eta_b,\eta_c)}}, \tag{5}$$

where each $V_{n,n}$ is the modulation extracted by TPC–FMD1,2, TPC–FMD3, and FMD1,2–FMD3 correlation, respectevily. This method is similar to the "3×2PC" method used by PHENIX [21, 56]. The

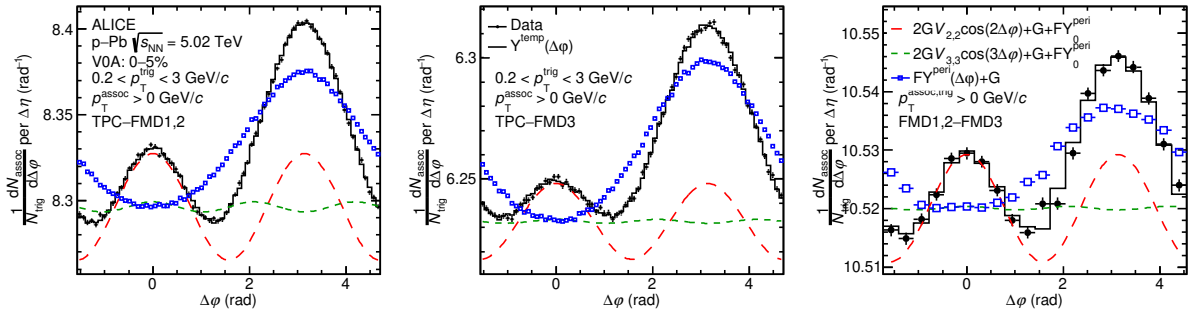

Figure 2: Projection of the correlation function of TPC–FMD1,2 (left), TPC–FMD3 (central), and FMD1,2–FMD3 (right) correlations in 0–5% p–Pb collisions with the template fit using Eq. (3). The open circle blue marker represents the scaled peripheral distribution plus the Flow baseline, G. The red and green dashed lines represent the second- and third-order components plus the baseline, respectively.

factorization breaks down if the event plane and/or the flow amplitude depend on pseudorapidity, for example because of initial longitudinal fluctuations or thermal fluctuations [57–62]. Therefore, the uncertainty due to those decorrelation effects is estimated by changing the η gap, as it will be discussed in Section 3.3.

Since the FMD is not a tracking detector, it is difficult to separate primary particles from secondary particles inside the FMD. Secondary particles are generated around the primary particle and might distort its distribution. The effects of secondary particles on the flow harmonics are estimated using MC simulations based on the AMPT and EPOS event generators [36, 63, 64]. The correction is performed based on the change in the reconstructed particle distribution after particle transport and interaction within the detector material from the original distribution. The correction factor is extracted as the ratio of the v_2 of primary particles over the v_2 of all reconstructed particles (i.e. including primary and secondary particles). In order to match the range of the FMD, which has acceptance down to $p_T = 0$, the charged-particle v_2 at midrapidity is extrapolated to $p_T = 0$ based on the data of the p_T spectrum and the p_T differential v_2 of charged-particles. The factor is about 0.86 for all four centralities.

3.3 Systematic uncertainties

The systematic uncertainties relate to the event selection, the track selection, the correction of secondary particles in the FMD, the material budget in the FMD, the choice of the peripheral event class for non-flow subtraction, the reference pseudorapidity choice of η_b, η_c to extract $v_2(\eta_a)$, and the jet modification. A systematic uncertainty is only assigned when the difference between the nominal data points and variations is statistically significant according to the Barlow criterium [65]. Table 2 shows the summary of systematic uncertainties for v_2, which depend on centrality and pseudorapidity as indicated by the range given. The uncertainty due to the event selection is investigated by changing the selection parameters for V0–FMD multiplicity correlations. The uncertainty slightly depends on centrality, and it is the largest in the 20–40% centrality class. The uncertainty due to track selection is evaluated by varying track selection parameters. This systematic uncertainty is 0.28–0.45% and is also the largest in the 20–40% centrality class. The systematic uncertainty related to the correction of the contamination by secondary particles is estimated using different event generators, EPOS and AMPT. The magnitude of collective-like signal in EPOS and AMPT is very different, and this check investigates how stable the correction is with respect to the magnitude of the flow. This uncertainty is found to be larger in the p-going direction than in the Pb-going direction. The number of secondary particles depends on the material budget in the ALICE environment. This systematic uncertainty is 2.3% estimated using MC simulations with increased or reduced material budget of the detector descriptions in GEANT simulation by $\pm 10\%$. Uncertainties as-

sociated with secondary correction and material budget are assigned only for the FMD acceptance. The systematic uncertainty of the peripheral event choice used for non-flow subtraction is estimated using the 80–100% event class instead of 60–100%. The systematic uncertainty on the reference pseudorapidity choice is investigated by changing the η gap between $\eta_{\rm b}$ and $\eta_{\rm c}$ to extract $v_2(\eta_{\rm a})$. The uncertainty ranges from 2.6% to 5.1% depending on the centrality and the choice of reference pseudorapidity. The shape of the jet is modified depending on the centrality. The uncertainty is evaluated by varying the away-side width of the peripheral collisions and is 0.8–2.7%. These systematic uncertainties are added in quadrature.

Table 2: The summary of systematic uncertainties, which is absolute value on v_2. The uncertainties take values within the given range depending on the centrality and pseudorapidity for each source.

Source of uncertainty	Systematic uncertainty (%)
Event selection	0.56–3.1%
Track selection	0.28–0.45%
Secondary correction	0.74–3.5%
Material budget	2.3%
Non-flow sub	0.76–4.6%
Jet modification	0.8–2.7%
η gap selection	2.6–5.1%
Total	3.9–8.3%

4 Results

The v_2 for charged-particles in a specific pseudorapidity region can be extracted using the template fit procedure and the three dihadron correlations of TPC–FMD1,2, TPC–FMD3, and FMD1,2–FMD3, as described in Section 3.2. The corresponding results of the $p_{\rm T}$-integrated v_2 as a function of η for the 0–5%, 5–10%, 10–20%, and 20–40% centrality classes are shown in Fig. 3. After applying the non-flow subtraction with the template fit approach, a non-zero v_2 is observed over a wide rapidity range for the first time in p–Pb collisions. The v_2 results in p–Pb collisions were measured previously for the pseudorapidity range of $|\eta| < 2$ by CMS [43, 44]. The v_2 measurements presented in this Letter significantly extend the measurements to a much wider pseudorapidity range, $-3.1 < \eta < 4.8$. This result confirms the emergence of anisotropic flow over a wide rapidity region, as in high-energy heavy-ion collisions [18]. In addition, the v_2 measurements show a significant pseudorapidity dependence for all four centrality classes. It is more prominent in the Pb-going direction (positive η) than in the p-going direction (negative η). Additionally, a stronger centrality dependence of v_2 is found in the Pb-going direction than in the p-going direction.

Previous $v_2(\eta)$ measurements showed that the magnitude of v_2 is correlated with charged-particle pseudorapidity density [45]; $v_2(\eta)$ increases with increasing multiplicity. However, $v_2(\eta)$ might not be linearly correlated with $\mathrm{d}N_{\rm ch}/\mathrm{d}\eta$ [42]. Figure 4 shows v_2 as a function of charged-particle multiplicity density for five different pseudorapidity regions and for different centrality classes: 0–5%, 5–10%, 10–20%, and 20–40%. Figure 4 demonstrates that the pseudorapidity dependence of v_2 is not just simply driven by the local multiplicity, v_2 independently depends on both η and $\mathrm{d}N_{\rm ch}/\mathrm{d}\eta$. In a fixed pseudorapidity range, v_2 depends on local multiplicity, but at fixed local multiplicity, there is still a significant dependence on the pseudorapidity.

Figure 5 shows the comparisons of v_2 in 0–5% p–Pb collisions and in 60–70% and 70–80% Pb–Pb collisions, where the multiplicity is similar in the Pb-going direction between the two collision systems [42, 66]. The charged-particle pseudorapidity density at $\eta \sim 3$ is about 60 in p–Pb collisions and 80 and 37 in 60–70% and 70–80% Pb–Pb collisions, respectively. Here, the results from Pb–Pb collisions

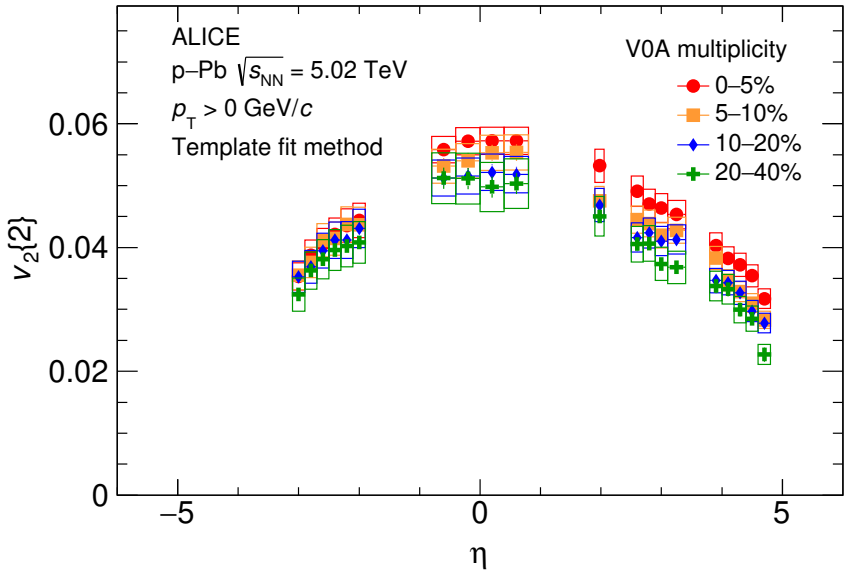

Figure 3: p_T-integrated $v_2\{2\}$ as a function of η in various centrality classes using the template fitting method. Boxes show the total systematic uncertainties.

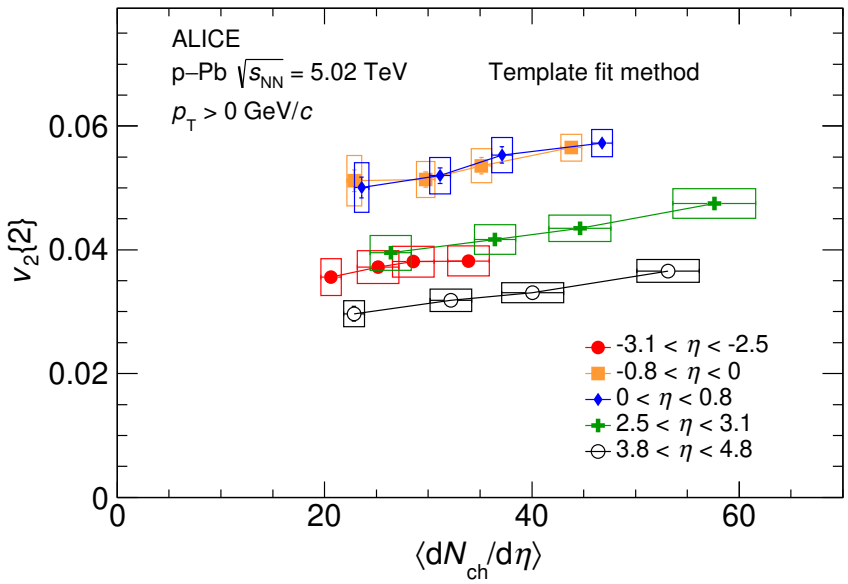

Figure 4: v_2 as a function of charged-particle pseudorapidity density for five different pseudorapidity regions.

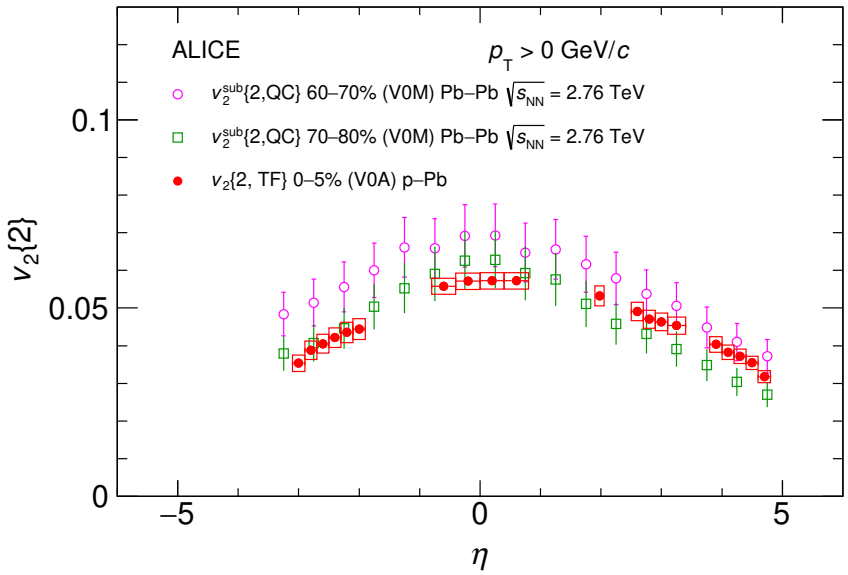

Figure 5: The $v_2(\eta)$ in central p–Pb collisions compared with $v_2(\eta)$ in peripheral Pb–Pb collisions with a compatible mean charged-particle multiplicity in Pb-going direction. The v_2 Pb–Pb results were obtained using the Q-cumulant method [18].

are based on the 2-particle cumulant method [18]. The v_2 results in p–Pb collisions are compatible with the v_2 in 60–70% and 70–80% Pb–Pb collisions over the entire η range within the sizable uncertainties of the Pb–Pb results. Somewhat unexpectedly, given the potential differences in the initial collision overlap geometry, it is observed that peripheral Pb–Pb collisions and central p–Pb collisions have comparable v_2 at similar multiplicities.

To further investigate the origin of the flow in small collision systems, the $v_2(\eta)$ measured in p–Pb collisions is compared with hydrodynamical calculations [67] in Fig. 6, and with the AMPT transport model in Fig. 7. The 3+1 hydrodynamical model employs 3D Glauber initial conditions, viscous hydrodynamics based on MUSIC, and the UrQMD model to simulate the dynamics in the hadronic phase. The shear viscosity and color string width in the transverse plane are adjusted to $\eta_T/(e+P) = 0.08$ and $\sigma_x = 0.4$ fm, respectively, to reproduce the mean transverse momentum of identified particles and the p_{T} dependence of charged-particle v_2 measured with the template fit procedure by ATLAS at midrapidity in p–Pb collisions at $\sqrt{s_{\mathrm{NN}}} = 5.02$ TeV [67]. The hydrodynamical model underestimates the pseudorapidity dependence of charged-particle multiplicity density when centrality is determined at forward pseudorapidity, while it is reproduced when centrality is determined at midrapidity [68]. The correlation between the multiplicities at forward and midrapidity is weaker in the model than in the data. In this model, v_2 mainly originates from the 3D initial geometry and develops in the course of the hydrodynamical evolution. The model describes the $v_2(\eta)$ measurement in 0–5% and 5–10%, while it somewhat overestimates the data in 10–20% and 20–40% at both forward and backward rapidity.

Similarly, Fig. 7 shows the comparisons with calculations by the AMPT model in the string-melting configuration. Unlike the hydrodynamical model, the AMPT with string melting is a transport model that produces collective behaviour microscopically by final-state scattering in both the partonic and hadronic phases. The $v_2(\eta)$ calculation from AMPT describes the data qualitatively in the 0–5% centrality class and reproduces the asymmetry between the Pb-going and p-going directions. However, the centrality dependence is less significant than observed in the data.

The comparisons between the $v_2(\eta)$ measurements and the calculations from the hydrodynamical and

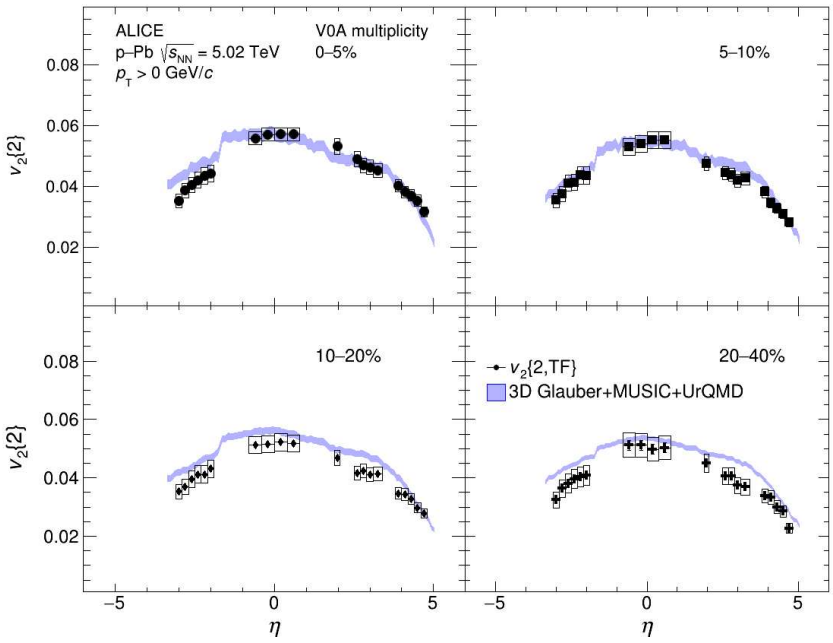

Figure 6: Pseudorapidity dependence of p_T integrated v_2. Comparison of the measured data (black circles) with a calculation by the hydrodynamical model (blue band) [67] for the 0–5% (top left), 5–10% (top right), 10–20% (bottom left), and 20–40% (bottom right) centrality classes.

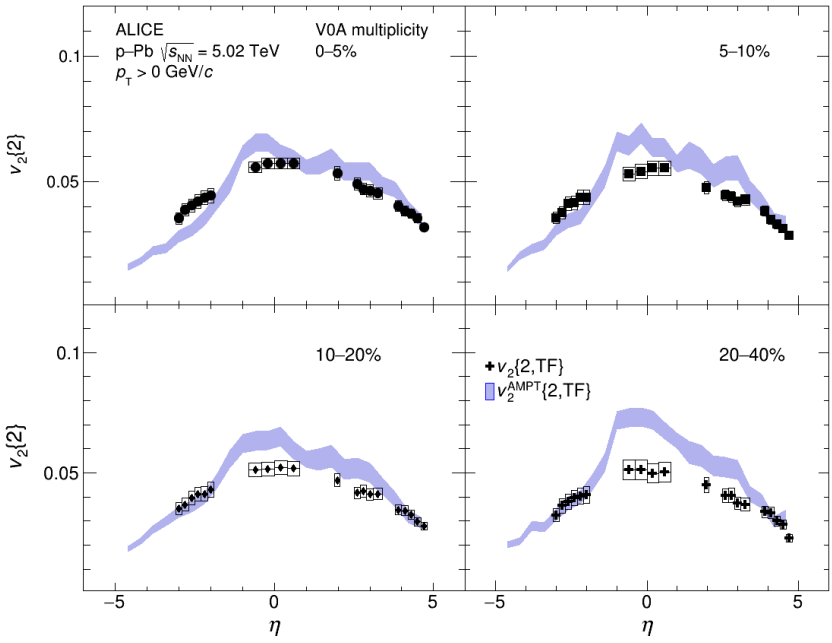

Figure 7: Pseudorapidity dependence of p_T integrated v_2. Comparison of the measured data (black circles) with a calculation by AMPT with the string-melting configuration (blue band) for 0–5% (top left), 5–10% (top right), 10–20% (bottom left), and 20–40% (bottom right) centrality class.

AMPT transport models suggest that strong final-state interactions are possibly the origin of a significant v_2 over a wide pseudorapidity range in small collision systems such as p–Pb collisions. Initial momentum anisotropy from Colour-Glass Condensate (CGC) could also play a role in high-multiplicity p–Pb collisions. However, a recent study using gluon saturation from the IP-Glasma model shows that the initial momentum anisotropy results to short-range correlation [69]. The observed finite v_2 extracted from ultra-long correlations will likely not be influenced by contributions from initial momentum anisotropy from CGC but more likely originates from the fluctuating initial geometry giving rise to final-state interactions.

5 Summary

In this Letter, the two-particle correlation function is presented as a function of $\Delta\eta$ and $\Delta\varphi$ in p–Pb collisions at $\sqrt{s_{\rm NN}} = 5.02$ TeV with ALICE. The "ridge" structure is observed up to a rapidity gap of 8 units between the trigger and the associate particles, in central events. A double-ridge structure is visible after the non-flow subtraction. The $p_{\rm T}$-integrated v_2 is extracted from the correlation function and presented as a function of pseudorapidity and centrality class. Non-zero v_2 is observed over a wide pseudorapidity range in central p–Pb collisions for the first time. The pseudorapidity dependence as well as its asymmetric shape of v_2 could be well explained by charged-particle multiplicity distributions. In addition, the $v_2(\eta)$ in p–Pb central events is comparable with the $v_2(\eta)$ in peripheral Pb–Pb collisions at similar multiplicity. Finally, both hydrodynamical [67] and AMPT transport model calculations [36] describe the data qualitatively over a wide pseudorapidity region. The comparison with the model calculations suggests the emergence of collective flow at very forward pseudorapidity ($|\eta| \sim 5$) region in p–Pb collisions, just like in high-energy heavy-ion collisions. The results suggest an important role of final-state interactions in developing anisotropic flow in small collision systems.

Acknowledgements

The ALICE Collaboration would like to thank all its engineers and technicians for their invaluable contributions to the construction of the experiment and the CERN accelerator teams for the outstanding performance of the LHC complex. The ALICE Collaboration gratefully acknowledges the resources and support provided by all Grid centres and the Worldwide LHC Computing Grid (WLCG) collaboration. The ALICE Collaboration acknowledges the following funding agencies for their support in building and running the ALICE detector: A. I. Alikhanyan National Science Laboratory (Yerevan Physics Institute) Foundation (ANSL), State Committee of Science and World Federation of Scientists (WFS), Armenia; Austrian Academy of Sciences, Austrian Science Fund (FWF): [M 2467-N36] and Nationalstiftung für Forschung, Technologie und Entwicklung, Austria; Ministry of Communications and High Technologies, National Nuclear Research Center, Azerbaijan; Conselho Nacional de Desenvolvimento Científico e Tecnológico (CNPq), Financiadora de Estudos e Projetos (Finep), Fundação de Amparo à Pesquisa do Estado de São Paulo (FAPESP) and Universidade Federal do Rio Grande do Sul (UFRGS), Brazil; Bulgarian Ministry of Education and Science, within the National Roadmap for Research Infrastructures 2020–2027 (object CERN), Bulgaria; Ministry of Education of China (MOEC) , Ministry of Science & Technology of China (MSTC) and National Natural Science Foundation of China (NSFC), China; Ministry of Science and Education and Croatian Science Foundation, Croatia; Centro de Aplicaciones Tecnológicas y Desarrollo Nuclear (CEADEN), Cubaenergía, Cuba; Ministry of Education, Youth and Sports of the Czech Republic, Czech Republic; The Danish Council for Independent Research — Natural Sciences, the VILLUM FONDEN and Danish National Research Foundation (DNRF), Denmark; Helsinki Institute of Physics (HIP), Finland; Commissariat à l'Energie Atomique (CEA) and Institut National de Physique Nucléaire et de Physique des Particules (IN2P3) and Centre National de la Recherche Scientifique (CNRS), France; Bundesministerium für Bildung und Forschung (BMBF) and GSI Helmholtzzentrum für Schwerionenforschung GmbH, Germany; General Secretariat for Research

and Technology, Ministry of Education, Research and Religions, Greece; National Research, Development and Innovation Office, Hungary; Department of Atomic Energy Government of India (DAE), Department of Science and Technology, Government of India (DST), University Grants Commission, Government of India (UGC) and Council of Scientific and Industrial Research (CSIR), India; National Research and Innovation Agency - BRIN, Indonesia; Istituto Nazionale di Fisica Nucleare (INFN), Italy; Japanese Ministry of Education, Culture, Sports, Science and Technology (MEXT) and Japan Society for the Promotion of Science (JSPS) KAKENHI, Japan; Consejo Nacional de Ciencia (CONACYT) y Tecnología, through Fondo de Cooperación Internacional en Ciencia y Tecnología (FONCICYT) and Dirección General de Asuntos del Personal Academico (DGAPA), Mexico; Nederlandse Organisatie voor Wetenschappelijk Onderzoek (NWO), Netherlands; The Research Council of Norway, Norway; Commission on Science and Technology for Sustainable Development in the South (COMSATS), Pakistan; Pontificia Universidad Católica del Perú, Peru; Ministry of Education and Science, National Science Centre and WUT ID-UB, Poland; Korea Institute of Science and Technology Information and National Research Foundation of Korea (NRF), Republic of Korea; Ministry of Education and Scientific Research, Institute of Atomic Physics, Ministry of Research and Innovation and Institute of Atomic Physics and University Politehnica of Bucharest, Romania; Ministry of Education, Science, Research and Sport of the Slovak Republic, Slovakia; National Research Foundation of South Africa, South Africa; Swedish Research Council (VR) and Knut & Alice Wallenberg Foundation (KAW), Sweden; European Organization for Nuclear Research, Switzerland; Suranaree University of Technology (SUT), National Science and Technology Development Agency (NSTDA) and National Science, Research and Innovation Fund (NSRF via PMU-B B05F650021), Thailand; Turkish Energy, Nuclear and Mineral Research Agency (TENMAK), Turkey; National Academy of Sciences of Ukraine, Ukraine; Science and Technology Facilities Council (STFC), United Kingdom; National Science Foundation of the United States of America (NSF) and United States Department of Energy, Office of Nuclear Physics (DOE NP), United States of America. In addition, individual groups or members have received support from: European Research Council, Strong 2020 - Horizon 2020 (grant nos. 950692, 824093), European Union; Academy of Finland (Center of Excellence in Quark Matter) (grant nos. 346327, 346328), Finland.

References

[1] **ALICE** Collaboration, "The ALICE experiment – A journey through QCD", arXiv:2211.04384 [nucl-ex].

[2] **PHOBOS** Collaboration, B. Alver *et al.*, "System size dependence of cluster properties from two-particle angular correlations in Cu+Cu and Au+Au collisions at $\sqrt{s_{\rm NN}} = 200$ GeV", *Phys. Rev. C* **81** (2010) 024904, arXiv:0812.1172 [nucl-ex].

[3] **STAR** Collaboration, J. Adams *et al.*, "Minijet deformation and charge-independent angular correlations on momentum subspace (η, φ) in Au–Au collisions at $\sqrt{s_{\rm NN}} = 130$ GeV", *Phys. Rev. C* **73** (2006) 064907, arXiv:nucl-ex/0411003.

[4] **PHOBOS** Collaboration, B. Alver *et al.*, "High transverse momentum triggered correlations over a large pseudorapidity acceptance in Au+Au collisions at $\sqrt{s_{\rm NN}} = 200$ GeV", *Phys. Rev. Lett.* **104** (2010) 062301, arXiv:0903.2811 [nucl-ex].

[5] **STAR** Collaboration, B. I. Abelev *et al.*, "Long range rapidity correlations and jet production in high energy nuclear collisions", *Phys. Rev. C* **80** (2009) 064912, arXiv:0909.0191 [nucl-ex].

[6] **STAR** Collaboration, G. Agakishiev *et al.*, "Anomalous centrality evolution of two-particle angular correlations from Au-Au collisions at $\sqrt{s_{\rm NN}} = 62$ and 200 GeV", *Phys. Rev. C* **86** (2012) 064902, arXiv:1109.4380 [nucl-ex].

[7] **CMS** Collaboration, S. Chatrchyan *et al.*, "Long-range and short-range dihadron angular correlations in central PbPb collisions at a nucleon-nucleon center of mass energy of 2.76 TeV", *JHEP* **07** (2011) 076, arXiv:1105.2438 [nucl-ex].

[8] **ALICE** Collaboration, K. Aamodt *et al.*, "Harmonic decomposition of two-particle angular correlations in Pb-Pb collisions at $\sqrt{s_{\rm NN}} = 2.76$ TeV", *Phys. Lett. B* **708** (2012) 249–264, arXiv:1109.2501 [nucl-ex].

[9] **CMS** Collaboration, S. Chatrchyan *et al.*, "Centrality dependence of dihadron correlations and azimuthal anisotropy harmonics in PbPb collisions at $\sqrt{s_{\rm NN}} = 2.76$ TeV", *Eur. Phys. J. C* **72** (2012) 2012, arXiv:1201.3158 [nucl-ex].

[10] **ATLAS** Collaboration, G. Aad *et al.*, "Measurement of the azimuthal anisotropy for charged particle production in $\sqrt{s_{\rm NN}} = 2.76$ TeV lead-lead collisions with the ATLAS detector", *Phys. Rev. C* **86** (2012) 014907, arXiv:1203.3087 [hep-ex].

[11] **ALICE** Collaboration, K. Aamodt *et al.*, "Higher harmonic anisotropic flow measurements of charged particles in Pb–Pb collisions at $\sqrt{s_{\rm NN}} = 2.76$ TeV", *Phys. Rev. Lett.* **107** (2011) 032301, arXiv:1105.3865 [nucl-ex].

[12] J.-Y. Ollitrault, "Anisotropy as a signature of transverse collective flow", *Phys. Rev. D* **46** (1992) 229–245.

[13] B. Alver and G. Roland, "Collision-geometry fluctuations and triangular flow in heavy-ion collisions", *Phys. Rev. C* **81** (2010) 054905.

[14] G. Denicol, A. Monnai, and B. Schenke, "Moving forward to constrain the shear viscosity of QCD matter", *Phys. Rev. Lett.* **116** (2016) 212301, arXiv:1512.01538 [nucl-th].

[15] C. Nonaka and K. Okamoto, "Phenomenological Analysis of High-Energy Heavy-Ion Collisions", *PoS* **KMI2017** (2017) 014.

[16] J. S. Moreland, J. E. Bernhard, and S. A. Bass, "Bayesian calibration of a hybrid nuclear collision model using p-Pb and Pb–Pb data at energies available at the CERN Large Hadron Collider", *Phys. Rev. C* **101** (2020) 024911, arXiv:1808.02106 [nucl-th].

[17] **PHOBOS** Collaboration, B. B. Back *et al.*, "Energy dependence of elliptic flow over a large pseudorapidity range in Au+Au collisions at RHIC", *Phys. Rev. Lett.* **94** (2005) 122303, arXiv:nucl-ex/0406021.

[18] **ALICE** Collaboration, J. Adam *et al.*, "Pseudorapidity dependence of the anisotropic flow of charged particles in Pb–Pb collisions at $\sqrt{s_{\rm NN}} = 2.76$ TeV", *Phys. Lett. B* **762** (2016) 376–388, arXiv:1605.02035 [nucl-ex].

[19] **PHENIX** Collaboration, A. Adare *et al.*, "Quadrupole Anisotropy in Dihadron Azimuthal Correlations in Central d+Au Collisions at $\sqrt{s_{\rm NN}} = 200$ GeV", *Phys. Rev. Lett.* **111** (2013) 212301, arXiv:1303.1794 [nucl-ex].

[20] **PHENIX** Collaboration, C. Aidala *et al.*, "Measurement of long-range angular correlations and azimuthal anisotropies in high-multiplicity p+Au collisions at $\sqrt{s_{\rm NN}} = 200$ GeV", *Phys. Rev. C* **95** (2017) 034910, arXiv:1609.02894 [nucl-ex].

[21] **PHENIX** Collaboration, U. A. Acharya *et al.*, "Kinematic dependence of azimuthal anisotropies in p+Au, d+Au, and ^{3}He+Au at $\sqrt{s_{\rm NN}} = 200$ GeV", *Phys. Rev. C* **105** (2022) 024901, arXiv:2107.06634 [hep-ex].

[22] **STAR** Collaboration, L. Adamczyk *et al.*, "Effect of event selection on jetlike correlation measurement in d+Au collisions at $\sqrt{s_{\rm NN}} = 200$ GeV", *Phys. Lett. B* **743** (2015) 333–339, arXiv:1412.8437 [nucl-ex].

[23] **STAR** Collaboration, M. I. Abdulhamid *et al.*, "Measurements of the Elliptic and Triangular Azimuthal Anisotropies in Central He3+Au, d+Au and p+Au Collisions at sNN=200 GeV", *Phys. Rev. Lett.* **130** (2023) 242301, arXiv:2210.11352 [nucl-ex].

[24] **CMS** Collaboration, V. Khachatryan *et al.*, "Observation of Long-Range Near-Side Angular Correlations in Proton-Proton Collisions at the LHC", *JHEP* **09** (2010) 091, arXiv:1009.4122 [hep-ex].

[25] **CMS** Collaboration, S. Chatrchyan *et al.*, "Observation of Long-Range Near-Side Angular Correlations in Proton-Lead Collisions at the LHC", *Phys. Lett. B* **718** (2013) 795–814, arXiv:1210.5482 [nucl-ex].

[26] **CMS** Collaboration, V. Khachatryan *et al.*, "Measurement of long-range near-side two-particle angular correlations in pp collisions at $\sqrt{s} = 13$ TeV", *Phys. Rev. Lett.* **116** (2016) 172302, arXiv:1510.03068 [nucl-ex].

[27] **CMS** Collaboration, V. Khachatryan *et al.*, "Evidence for collectivity in pp collisions at the LHC", *Phys. Lett. B* **765** (2017) 193–220, arXiv:1606.06198 [nucl-ex].

[28] **ALICE** Collaboration, B. Abelev *et al.*, "Long-range angular correlations on the near and away side in p-Pb collisions at $\sqrt{s_{\rm NN}} = 5.02$ TeV", *Phys. Lett. B* **719** (2013) 29–41, arXiv:1212.2001 [nucl-ex].

[29] **ALICE** Collaboration, B. Abelev *et al.*, "Long-range angular correlations of π, K and p in p-Pb collisions at $\sqrt{s_{\rm NN}} = 5.02$ TeV", *Phys. Lett. B* **726** (2013) 164–177, arXiv:1307.3237 [nucl-ex].

[30] **ATLAS** Collaboration, G. Aad *et al.*, "Observation of Associated Near-Side and Away-Side Long-Range Correlations in $\sqrt{s_{\rm NN}} = 5.02$ TeV Proton-Lead Collisions with the ATLAS Detector", *Phys. Rev. Lett.* **110** (2013) 182302, arXiv:1212.5198 [hep-ex].

[31] **ATLAS** Collaboration, G. Aad *et al.*, "Measurement of long-range pseudorapidity correlations and azimuthal harmonics in $\sqrt{s_{\rm NN}} = 5.02$ TeV proton-lead collisions with the ATLAS detector", *Phys. Rev. C* **90** (2014) 044906, arXiv:1409.1792 [hep-ex].

[32] **CMS** Collaboration, A. M. Sirunyan *et al.*, "Elliptic flow of charm and strange hadrons in high-multiplicity pPb collisions at $\sqrt{s_{\rm NN}} = 8.16$ TeV", *Phys. Rev. Lett.* **121** (2018) 082301, arXiv:1804.09767 [hep-ex].

[33] P. Bozek and W. Broniowski, "Collective dynamics in high-energy proton-nucleus collisions", *Phys. Rev. C* **88** (2013) 014903, arXiv:1304.3044 [nucl-th].

[34] R. D. Weller and P. Romatschke, "One fluid to rule them all: viscous hydrodynamic description of event-by-event central p+p, p+Pb and Pb+Pb collisions at $\sqrt{s} = 5.02$ TeV", *Phys. Lett. B* **774** (2017) 351–356, arXiv:1701.07145 [nucl-th].

[35] J. L. Albacete *et al.*, "Predictions for p+Pb Collisions at $\sqrt{s_{\rm NN}} = 5$ TeV", *Int. J. Mod. Phys. E* **22** (2013) 1330007, arXiv:1301.3395 [hep-ph].

[36] J. L. Albacete *et al.*, "Predictions for p+Pb Collisions at $\sqrt{s_{NN}} = 5$ TeV: Comparison with Data", *Int. J. Mod. Phys. E* **25** (2016) 1630005, arXiv:1605.09479 [hep-ph].

[37] Y. Zhou, X. Zhu, P. Li, and H. Song, "Investigation of possible hadronic flow in $\sqrt{s_{NN}} = 5.02$ TeV $p-Pb$ collisions", *Phys. Rev. C* **91** (2015) 064908, arXiv:1503.06986 [nucl-th].

[38] W. Zhao, Y. Zhou, H. Xu, W. Deng, and H. Song, "Hydrodynamic collectivity in proton–proton collisions at 13 TeV", *Phys. Lett. B* **780** (2018) 495–500, arXiv:1801.00271 [nucl-th].

[39] B. Schenke, C. Shen, and P. Tribedy, "Hybrid Color Glass Condensate and hydrodynamic description of the Relativistic Heavy Ion Collider small system scan", *Phys. Lett. B* **803** (2020) 135322, arXiv:1908.06212 [nucl-th].

[40] Y. Kanakubo, Y. Tachibana, and T. Hirano, "Interplay between core and corona components in high-energy nuclear collisions", *Phys. Rev. C* **105** (2022) 024905, arXiv:2108.07943 [nucl-th].

[41] M. Nie, L. Yi, G. Ma, and J. Jia, "Influence of initial-state momentum anisotropy on the final-state collectivity in small collision systems", *Phys. Rev. C* **100** (2019) 064905, arXiv:1906.01422 [nucl-th].

[42] **ALICE** Collaboration, S. Acharya *et al.*, "System-size dependence of the charged-particle pseudorapidity density at $\sqrt{s_{\rm NN}} = 5.02$ TeV for pp, p-Pb, and Pb-Pb collisions", *Phys. Lett. B* **845** (2023) 137730, arXiv:2204.10210 [nucl-ex].

[43] **CMS** Collaboration, V. Khachatryan *et al.*, "Pseudorapidity dependence of long-range two-particle correlations in pPb collisions at $\sqrt{s_{\rm NN}} = 5.02$ TeV", *Phys. Rev. C* **96** (2017) 014915, arXiv:1604.05347 [nucl-ex].

[44] **CMS** Collaboration, A. M. Sirunyan *et al.*, "Pseudorapidity and transverse momentum dependence of flow harmonics in pPb and PbPb collisions", *Phys. Rev. C* **98** (2018) 044902, arXiv:1710.07864 [nucl-ex].

[45] **PHENIX** Collaboration, A. Adare *et al.*, "Pseudorapidity Dependence of Particle Production and Elliptic Flow in Asymmetric Nuclear Collisions of p+Al, p+Au, d+Au, and ^{3}He+Au at $\sqrt{s_{\rm NN}} = 200$ GeV", *Phys. Rev. Lett.* **121** (2018) 222301, arXiv:1807.11928 [nucl-ex].

[46] **PHENIX** Collaboration, C. Aidala *et al.*, "Measurements of azimuthal anisotropy and charged-particle multiplicity in d+Au collisions at $\sqrt{s_{\rm NN}} = 200$, 62.4, 39, and 19.6 GeV", *Phys. Rev. C* **96** (2017) 064905, arXiv:1708.06983 [nucl-ex].

[47] P. Bozek and W. Broniowski, "Collective flow in ultrarelativistic ^{3}He-Au collisions", *Phys. Lett. B* **739** (2014) 308–312, arXiv:1409.2160 [nucl-th].

[48] **ALICE** Collaboration, K. Aamodt *et al.*, "The ALICE experiment at the CERN LHC", *JINST* **3** (2008) S08002.

[49] **ALICE** Collaboration, B. B. Abelev *et al.*, "Performance of the ALICE Experiment at the CERN LHC", *Int. J. Mod. Phys. A* **29** (2014) 1430044, arXiv:1402.4476 [nucl-ex].

[50] **ALICE** Collaboration, B. Abelev *et al.*, "Pseudorapidity density of charged particles in p + Pb collisions at $\sqrt{s_{\rm NN}} = 5.02$ TeV", *Phys. Rev. Lett.* **110** (2013) 032301, arXiv:1210.3615 [nucl-ex].

[51] **ALICE** Collaboration, B. Abelev *et al.*, "Centrality Dependence of Charged Particle Production at Large Transverse Momentum in Pb–Pb Collisions at $\sqrt{s_{\rm NN}} = 2.76$ TeV", *Phys. Lett. B* **720** (2013) 52–62, arXiv:1208.2711 [hep-ex].

[52] S. Roesler, R. Engel, and J. Ranft, "The Monte Carlo event generator DPMJET-III", in *International Conference on Advanced Monte Carlo for Radiation Physics, Particle Transport Simulation and Applications (MC 2000)*, pp. 1033–1038. 12, 2000. arXiv:hep-ph/0012252.

[53] R. Brun, F. Bruyant, F. Carminati, S. Giani, M. Maire, A. McPherson, G. Patrick, and L. Urban, *GEANT: Detector Description and Simulation Tool; Oct 1994*. CERN Program Library. CERN, Geneva, 1993. https://cds.cern.ch/record/1082634. Long Writeup W5013.

[54] **ATLAS** Collaboration, G. Aad *et al.*, "Observation of Long-Range Elliptic Azimuthal Anisotropies in $\sqrt{s}$ =13 and 2.76 TeV pp Collisions with the ATLAS Detector", *Phys. Rev. Lett.* **116** (2016) 172301, arXiv:1509.04776 [hep-ex].

[55] **ATLAS** Collaboration, M. Aaboud *et al.*, "Measurements of long-range azimuthal anisotropies and associated Fourier coefficients for pp collisions at $\sqrt{s} = 5.02$ and 13 TeV and p+Pb collisions at $\sqrt{s_{\rm NN}} = 5.02$ TeV with the ATLAS detector", *Phys. Rev. C* **96** (2017) 024908, arXiv:1609.06213 [nucl-ex].

[56] **PHENIX** Collaboration, N. J. Abdulameer *et al.*, "Measurements of second-harmonic Fourier coefficients from azimuthal anisotropies in $p+p$, p+Au, d+Au, and ^{3}He+Au collisions at $\sqrt{s_{\rm NN}} = 200$GeV", *Phys. Rev. C* **107** (2023) 024907, arXiv:2203.09894 [nucl-ex].

[57] **ATLAS** Collaboration, M. Aaboud *et al.*, "Measurement of longitudinal flow decorrelations in Pb+Pb collisions at $\sqrt{s_{\rm NN}} = 2.76$ and 5.02 TeV with the ATLAS detector", *Eur. Phys. J. C* **78** (2018) 142, arXiv:1709.02301 [nucl-ex].

[58] **ATLAS** Collaboration, G. Aad *et al.*, "Longitudinal Flow Decorrelations in Xe+Xe Collisions at $\sqrt{s_{\rm NN}} = 5.44$ TeV with the ATLAS Detector", *Phys. Rev. Lett.* **126** (2021) 122301, arXiv:2001.04201 [nucl-ex].

[59] **CMS** Collaboration, V. Khachatryan *et al.*, "Evidence for transverse momentum and pseudorapidity dependent event plane fluctuations in PbPb and pPb collisions", *Phys. Rev. C* **92** (2015) 034911, arXiv:1503.01692 [nucl-ex].

[60] A. Sakai, K. Murase, and T. Hirano, "Effects of hydrodynamic and initial longitudinal fluctuations on rapidity decorrelation of collective flow", *Phys. Lett. B* **829** (2022) 137053, arXiv:2111.08963 [nucl-th].

[61] P. Bozek and W. Broniowski, "Longitudinal decorrelation measures of flow magnitude and event-plane angles in ultrarelativistic nuclear collisions", *Phys. Rev. C* **97** (2018) 034913, arXiv:1711.03325 [nucl-th].

[62] P. Bozek and W. Broniowski, "The torque effect and fluctuations of entropy deposition in rapidity in ultra-relativistic nuclear collisions", *Phys. Lett. B* **752** (2016) 206–211, arXiv:1506.02817 [nucl-th].

[63] Z.-W. Lin, C. M. Ko, B.-A. Li, B. Zhang, and S. Pal, "A Multi-phase transport model for relativistic heavy ion collisions", *Phys. Rev. C* **72** (2005) 064901, arXiv:nucl-th/0411110.

[64] T. Pierog, I. Karpenko, J. M. Katzy, E. Yatsenko, and K. Werner, "EPOS LHC: Test of collective hadronization with data measured at the CERN Large Hadron Collider", *Phys. Rev. C* **92** (2015) 034906, arXiv:1306.0121 [hep-ph].

[65] R. Barlow, "Systematic errors: Facts and fictions", in *Conference on Advanced Statistical Techniques in Particle Physics*, pp. 134–144. 7, 2002. arXiv:hep-ex/0207026.

[66] **ALICE** Collaboration, J. Adam *et al.*, "Centrality evolution of the charged–particle pseudorapidity density over a broad pseudorapidity range in Pb–Pb collisions at $\sqrt{s_{\rm NN}} = 2.76$ TeV", *Phys. Lett. B* **754** (2016) 373–385, arXiv:1509.07299 [nucl-ex].

[67] W. Zhao, C. Shen, and B. Schenke, "Collectivity in Ultraperipheral Pb+Pb Collisions at the Large Hadron Collider", *Phys. Rev. Lett.* **129** (2022) 252302, arXiv:2203.06094 [nucl-th].

[68] C. Shen and B. Schenke, "Longitudinal dynamics and particle production in relativistic nuclear collisions", *Phys. Rev. C* **105** (2022) 064905, arXiv:2203.04685 [nucl-th].

[69] B. Schenke, S. Schlichting, and P. Singh, "Rapidity dependence of initial state geometry and momentum correlations in p+Pb collisions", *Phys. Rev. D* **105** (2022) 094023, arXiv:2201.08864 [nucl-th].

[70] **ATLAS** Collaboration, M. Aaboud *et al.*, "Correlated long-range mixed-harmonic fluctuations measured in pp, p+Pb and low-multiplicity Pb+Pb collisions with the ATLAS detector", *Phys. Lett. B* **789** (2019) 444–471, arXiv:1807.02012 [nucl-ex].

A Non-flow subtraction with the improved-template-fit method and peripheral subtraction procedure

To examine the robustness of the observation, two different derived template-fit methods for non-flow suppression are employed: the zero-yield-at-minimum (ZYAM) and the improved-template-fit method [54, 70]. Henceforth, the peripheral subtraction will denote the ZYAM template-fit method. The term of $FY^{\rm peri}(\Delta\varphi)$ in Eq. (3) is substituted by $FY^{\rm peri}(\Delta\varphi) - Y_0$, where Y_0 is the baseline of the correlation function in peripheral events, which is determined at $\Delta\varphi \sim 0$. The peripheral subtraction method assumes that the 2nd-order modulation is zero when the multiplicity is zero. An improved-template-fit method was developed to estimate the non-flow effects in peripheral collisions more realistically. This method assumes that there are no flow components in the peripheral events. On the other hand, this procedure takes into account the residual flow components in peripheral events. The flow harmonics in the second-most peripheral events are extracted by the template fit using the correlation function in the most peripheral events given by

$$Y^{\rm peri}(\Delta\varphi) = Y_{\text{non-flow}}(\Delta\varphi) + G^{\rm peri}\{1 + 2\sum_{n=2}^{3} v_{n,n}^{\rm peri}\cos(n\Delta\varphi)\}, \tag{A.1}$$

where $Y^{\rm peri}(\Delta\varphi)$ and $Y_{\rm non-flow}(\Delta\varphi)$ are the correlation functions in the second-most and the most peripheral events, respectively. By substituting Eq. (A.1) with Eq. (3), it can be seen that

$$Y(\Delta\varphi) = FY_{\text{non-flow}}(\Delta\varphi) + (G^{\rm tmp} + FG^{\rm peri})\{1 + 2\sum_{n=2}^{3}\frac{G^{\rm tmp}v_{n,n}^{\rm tmp} + FG^{\rm peri}v_{n,n}^{\rm peri}}{G^{\rm tmp} + FG^{\rm peri}}\cos(n\Delta\varphi)\}. \tag{A.2}$$

Finally, the non-flow subtracted flow coefficient from the improved-template-fit method, $v_{n,n}^{\rm imp}$, can be obtained as

$$v_{n,n}^{\rm imp} = v_{n,n}^{\rm tmp} - \frac{FG^{\rm peri}}{G^{\rm tmp} + FG^{\rm peri}}(v_{n,n}^{\rm tmp} - v_{n,n}^{\rm peri}). \tag{A.3}$$

Figure A.1 shows the $p_{\rm T}$-integrated v_2 as a function of η with two different non-flow suppression methods for 0–5%, 5–10%, 10–20%, and 20–40% p–Pb collisions. The improved-template-fit method, which considers v_2 in peripheral collisions, gives smaller v_2 than the template-fit method; however, the difference is insignificant for the presented pseudorapidity regions. The effect of the second-order component in the peripheral collision is small. The result of v_2 from the peripheral subtraction method, which assumes no elliptic flow in the peripheral collision, is about 15% smaller than the template procedure for the 0–5% centrality class. Regardless of which non-flow subtraction method is applied, non-zero v_2 results are observed for the entire presented pseudorapidity region with more than 5-σ confidence, further confirming the observations of anisotropic flow in high-multiplicity p–Pb collisions. Figure A.2 shows the v_2 as a function of local charged-particle density for five different pseudorapidity regions with the peripheral subtraction (left) and the improved-template-fit (right) methods. Similar to the template fit results shown in Fig. 4, v_2 from peripheral subtraction and improved-templated-fit methods show a charged multiplicity density dependence. Fig. A.3 also shows the comparisons of v_2 in 0–5% central p–Pb collisions and in peripheral Pb–Pb collisions with the improved-template-fit method and the peripheral subtraction. The v_2 of the improved-template-fit method is comparable to the v_2 in peripheral Pb–Pb collisions with similar multiplicity at forward rapidity as well as the v_2 of the template fit. At the same time, the v_2 result from the peripheral subtraction is consistent with the results in Pb–Pb in the Pb-going direction within the uncertainty; however, it is smaller in the p-going direction. Figure A.4 compares the AMPT calculation and the results with the improved-template-fit and the peripheral subtraction methods. Similar to the experimental measurements, improved-template-fit and peripheral subtraction methods are also applied in these AMPT calculations. It is found that the AMPT calculations also exhibit the differences in v_2 from the improved-template-fit method and the peripheral subtraction, just as the data. This is because

both template-fit and improved-template-fit methods consider possible flow generated in peripheral collisions, which is the case in the AMPT model, while such flow contributions are treated as non-flow and subtracted in the peripheral subtraction method.

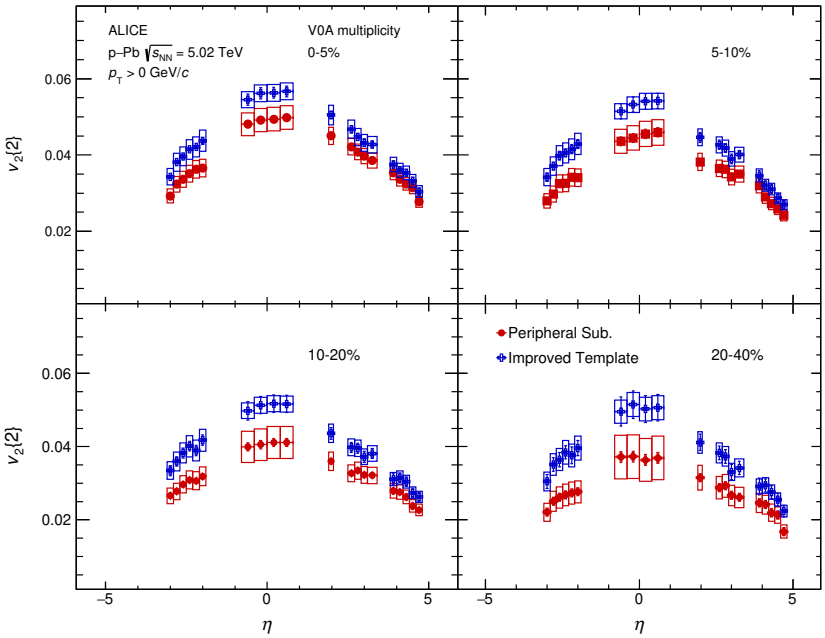

Figure A.1: p_T-integrated $v_2\{2\}$ as a function of η in various centrality classes using the improved-template-fit method, and the peripheral subtraction method.

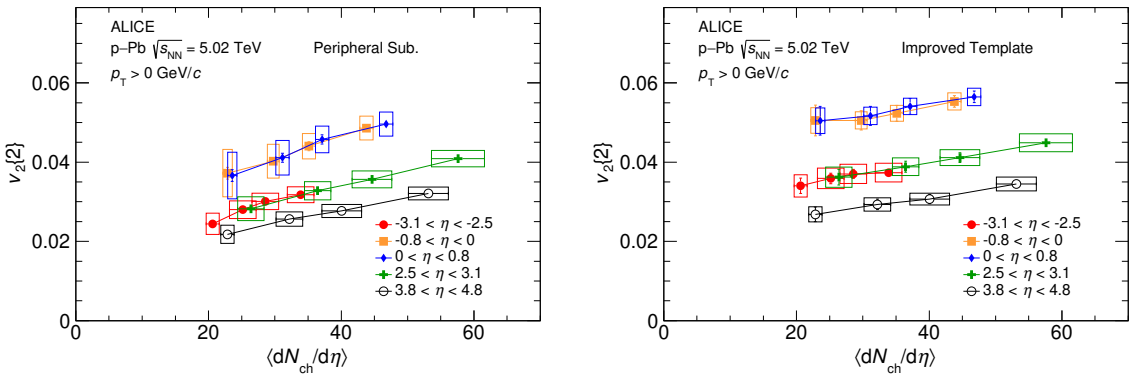

Figure A.2: v_2 as a function of charged particle density for five different pseudorapidity regions with the peripheral subtraction (left) and the improved template method (right).

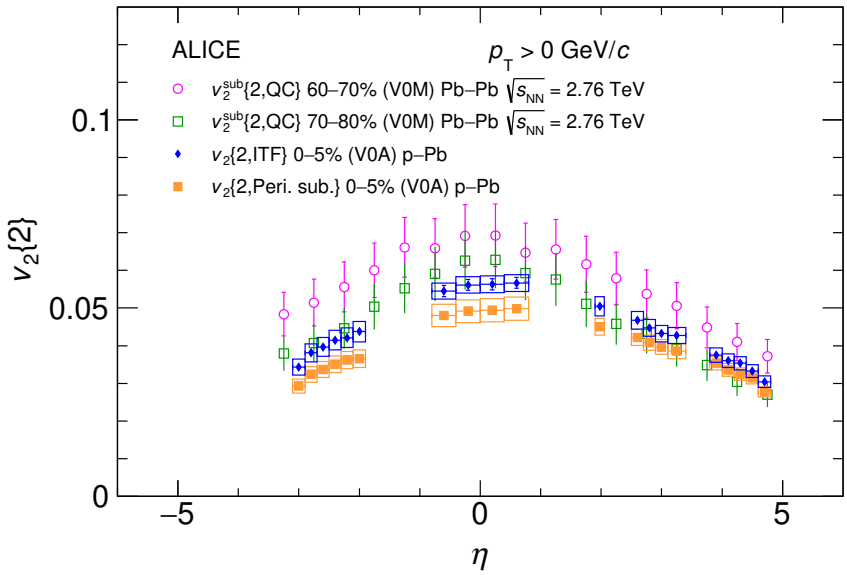

Figure A.3: Pseudorapidity dependence of p_T-integrated v_2 as measured in peripheral Pb–Pb collisions and central p–Pb collisions. The Pb–Pb results were obtained with the Q-cumulant method [18]. The p–Pb results were obtained with the improved-template-fit and peripheral subtraction methods.

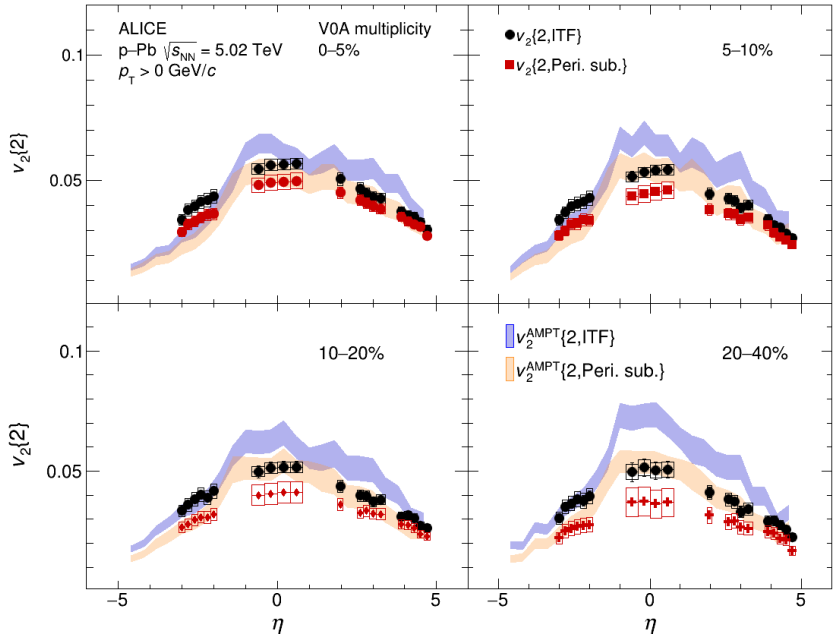

Figure A.4: Pseudorapidity dependence of p_T-integrated v_2 as measured in different p–Pb centrality classes and as obtained from the AMPT calculation with the string melting configuration. The v_2 were extracted using the improved-template-fit method and the peripheral subtraction.

B The ALICE Collaboration

S. Acharya [126], D. Adamová [86], G. Aglieri Rinella [33], M. Agnello [30], N. Agrawal [51], Z. Ahammed [134], S. Ahmad[16], S.U. Ahn [71], I. Ahuja [38], A. Akindinov [142], M. Al-Turany [97], D. Aleksandrov [142], B. Alessandro [56], H.M. Alfanda [6], R. Alfaro Molina [67], B. Ali [16], A. Alici [26], N. Alizadehvandchali [115], A. Alkin [33], J. Alme [21], G. Alocco [52], T. Alt [64], A.R. Altamura [50], I. Altsybeev [95], M.N. Anaam [6], C. Andrei [46], N. Andreou [114], A. Andronic [137], V. Anguelov [94], F. Antinori [54], P. Antonioli [51], N. Apadula [74], L. Aphecetche [103], H. Appelshäuser [64], C. Arata [73], S. Arcelli [26], M. Aresti [23], R. Arnaldi [56], J.G.M.C.A. Arneiro [110], I.C. Arsene [20], M. Arslandok [139], A. Augustinus [33], R. Averbeck [97], M.D. Azmi[16], H. Baba[123], A. Badalà [53], J. Bae [104], Y.W. Baek [41], X. Bai [119], R. Bailhache [64], Y. Bailung [48], A. Balbino [30], A. Baldisseri [129], B. Balis [2], D. Banerjee [4], Z. Banoo [91], R. Barbera [27], F. Barile [32], L. Barioglio [95], M. Barlou[78], B. Barman[42], G.G. Barnaföldi [138], L.S. Barnby [85], V. Barret [126], L. Barreto [110], C. Bartels [118], K. Barth [33], E. Bartsch [64], N. Bastid [126], S. Basu [75], G. Batigne [103], D. Battistini [95], B. Batyunya [143], D. Bauri[47], J.L. Bazo Alba [101], I.G. Bearden [83], C. Beattie [139], P. Becht [97], D. Behera [48], I. Belikov [128], A.D.C. Bell Hechavarria [137], F. Bellini [26], R. Bellwied [115], S. Belokurova [142], Y.A.V. Beltran [45], G. Bencedi [138], S. Beole [25], Y. Berdnikov [142], A. Berdnikova [94], L. Bergmann [94], M.G. Besoiu [63], L. Betev [33], P.P. Bhaduri [134], A. Bhasin [91], M.A. Bhat [4], B. Bhattacharjee [42], L. Bianchi [25], N. Bianchi [49], J. Bielčík [36], J. Bielčíková [86], J. Biernat [107], A.P. Bigot [128], A. Bilandzic [95], G. Biro [138], S. Biswas [4], N. Bize [103], J.T. Blair [108], D. Blau [142], M.B. Blidaru [97], N. Bluhme[39], C. Blume [64], G. Boca [22,55], F. Bock [87], T. Bodova [21], A. Bogdanov[142], S. Boi [23], J. Bok [58], L. Boldizsár [138], M. Bombara [38], P.M. Bond [33], G. Bonomi [133,55], H. Borel [129], A. Borissov [142], A.G. Borquez Carcamo [94], H. Bossi [139], E. Botta [25], Y.E.M. Bouziani [64], L. Bratrud [64], P. Braun-Munzinger [97], M. Bregant [110], M. Broz [36], G.E. Bruno [96,32], M.D. Buckland [24], D. Budnikov [142], H. Buesching [64], S. Bufalino [30], P. Buhler [102], N. Burmasov [142], Z. Buthelezi [68,122], A. Bylinkin [21], S.A. Bysiak[107], M. Cai [6], H. Caines [139], A. Caliva [29], E. Calvo Villar [101], J.M.M. Camacho [109], P. Camerini [24], F.D.M. Canedo [110], M. Carabas [125], A.A. Carballo [33], F. Carnesecchi [33], R. Caron [127], L.A.D. Carvalho [110], J. Castillo Castellanos [129], F. Catalano [33,25], C. Ceballos Sanchez [143], I. Chakaberia [74], P. Chakraborty [47], S. Chandra [134], S. Chapeland [33], M. Chartier [118], S. Chattopadhyay [134], S. Chattopadhyay [99], T.G. Chavez [45], T. Cheng [97,6], C. Cheshkov [127], B. Cheynis [127], V. Chibante Barroso [33], D.D. Chinellato [111], E.S. Chizzali [I,95], J. Cho [58], S. Cho [58], P. Chochula [33], D. Choudhury[42], P. Christakoglou [84], C.H. Christensen [83], P. Christiansen [75], T. Chujo [124], M. Ciacco [30], C. Cicalo [52], F. Cindolo [51], M.R. Ciupek[97], G. Clai[II,51], F. Colamaria [50], J.S. Colburn[100], D. Colella [96,32], M. Colocci [26], M. Concas [III,33], G. Conesa Balbastre [73], Z. Conesa del Valle [130], G. Contin [24], J.G. Contreras [36], M.L. Coquet [129], P. Cortese [132,56], M.R. Cosentino [112], F. Costa [33], S. Costanza [22,55], C. Cot [130], J. Crkovská [94], P. Crochet [126], R. Cruz-Torres [74], P. Cui [6], A. Dainese [54], M.C. Danisch [94], A. Danu [63], P. Das [80], P. Das [4], S. Das [4], A.R. Dash [137], S. Dash [47], R.M.H. David[45], A. De Caro [29], G. de Cataldo [50], J. de Cuveland[39], A. De Falco [23], D. De Gruttola [29], N. De Marco [56], C. De Martin [24], S. De Pasquale [29], R. Deb [133], R. Del Grande [95], L. Dello Stritto [29], W. Deng [6], P. Dhankher [19], D. Di Bari [32], A. Di Mauro [33], B. Diab [129], R.A. Diaz [143,7], T. Dietel [113], Y. Ding [6], J. Ditzel [64], R. Divià [33], D.U. Dixit [19], Ø. Djuvsland[21], U. Dmitrieva [142], A. Dobrin [63], B. Dönigus [64], J.M. Dubinski [135], A. Dubla [97], S. Dudi [90], P. Dupieux [126], M. Durkac[106], N. Dzalaiova[13], T.M. Eder [137], R.J. Ehlers [74], F. Eisenhut [64], R. Ejima[92], D. Elia [50], B. Erazmus [103], F. Ercolessi [26], B. Espagnon [130], G. Eulisse [33], D. Evans [100], S. Evdokimov [142], L. Fabbietti [95], M. Faggin [28], J. Faivre [73], F. Fan [6], W. Fan [74], A. Fantoni [49], M. Fasel [87], A. Feliciello [56], G. Feofilov [142], A. Fernández Téllez [45], L. Ferrandi [110], M.B. Ferrer [33], A. Ferrero [129], C. Ferrero [56], A. Ferretti [25], V.J.G. Feuillard [94], V. Filova [36], D. Finogeev [142], F.M. Fionda [52], E. Flatland[33], F. Flor [115], A.N. Flores [108], S. Foertsch [68], I. Fokin [94], S. Fokin [142], E. Fragiacomo [57], E. Frajna [138], U. Fuchs [33], N. Funicello [29], C. Furget [73], A. Furs [142], T. Fusayasu [98], J.J. Gaardhøje [83], M. Gagliardi [25], A.M. Gago [101], T. Gahlaut[47], C.D. Galvan [109], D.R. Gangadharan [115], P. Ganoti [78], C. Garabatos [97], A.T. Garcia [130], J.R.A. Garcia [45], E. Garcia-Solis [9], C. Gargiulo [33], P. Gasik [97], A. Gautam [117], M.B. Gay Ducati [66], M. Germain [103], A. Ghimouz[124], C. Ghosh[134], M. Giacalone [51], G. Gioachin [30], P. Giubellino [97,56], P. Giubilato [28], A.M.C. Glaenzer [129], P. Glässel [94], E. Glimos [121], D.J.Q. Goh[76], V. Gonzalez [136], P. Gordeev[142], M. Gorgon [2], K. Goswami [48], S. Gotovac[34], V. Grabski [67], L.K. Graczykowski [135], E. Grecka [86], A. Grelli [59], C. Grigoras [33], V. Grigoriev [142], S. Grigoryan [143,1], F. Grosa [33], J.F. Grosse-Oetringhaus [33], R. Grosso [97], D. Grund [36], N.A. Grunwald[94], G.G. Guardiano [111], R. Guernane [73], M. Guilbaud [103], K. Gulbrandsen [83], T. Gündem [64], T. Gunji [123],

W. Guo [6], A. Gupta [91], R. Gupta [91], R. Gupta [48], S.P. Guzman [45], K. Gwizdziel [135], L. Gyulai [138], C. Hadjidakis [130], F.U. Haider [91], S. Haidlova [36], H. Hamagaki [76], A. Hamdi [74], Y. Han [140], B.G. Hanley [136], R. Hannigan [108], J. Hansen [75], M.R. Haque [135], J.W. Harris [139], A. Harton [9], H. Hassan [116], D. Hatzifotiadou [51], P. Hauer [43], L.B. Havener [139], S.T. Heckel [95], E. Hellbär [97], H. Helstrup [35], M. Hemmer [64], T. Herman [36], G. Herrera Corral [8], F. Herrmann[137], S. Herrmann [127], K.F. Hetland [35], B. Heybeck [64], H. Hillemanns [33], B. Hippolyte [128], F.W. Hoffmann [70], B. Hofman [59], G.H. Hong [140], M. Horst [95], A. Horzyk[2], Y. Hou [6], P. Hristov [33], C. Hughes [121], P. Huhn[64], L.M. Huhta [116], T.J. Humanic [88], A. Hutson [115], D. Hutter [39], R. Ilkaev[142], H. Ilyas [14], M. Inaba [124], G.M. Innocenti [33], M. Ippolitov [142], A. Isakov [84,86], T. Isidori [117], M.S. Islam [99], M. Ivanov [97], M. Ivanov[13], V. Ivanov [142], K.E. Iversen [75], M. Jablonski [2], B. Jacak [74], N. Jacazio [26], P.M. Jacobs [74], S. Jadlovska[106], J. Jadlovsky[106], S. Jaelani [82], C. Jahnke [110], M.J. Jakubowska [135], M.A. Janik [135], T. Janson[70], S. Ji [17], S. Jia [10], A.A.P. Jimenez [65], F. Jonas [87], D.M. Jones [118], J.M. Jowett [33,97], J. Jung [64], M. Jung [64], A. Junique [33], A. Jusko [100], M.J. Kabus [33,135], J. Kaewjai[105], P. Kalinak [60], A.S. Kalteyer [97], A. Kalweit [33], V. Kaplin [142], A. Karasu Uysal [72], D. Karatovic [89], O. Karavichev [142], T. Karavicheva [142], P. Karczmarczyk [135], E. Karpechev [142], U. Kebschull [70], R. Keidel [141], D.L.D. Keijdener[59], M. Keil [33], B. Ketzer [43], S.S. Khade [48], A.M. Khan [119], S. Khan [16], A. Khanzadeev [142], Y. Kharlov [142], A. Khatun [117], A. Khuntia [36], B. Kileng [35], B. Kim [104], C. Kim [17], D.J. Kim [116], E.J. Kim [69], J. Kim [140], J.S. Kim [41], J. Kim [58], J. Kim [69], M. Kim [19], S. Kim [18], T. Kim [140], K. Kimura [92], S. Kirsch [64], I. Kisel [39], S. Kiselev [142], A. Kisiel [135], J.P. Kitowski [2], J.L. Klay [5], J. Klein [33], S. Klein [74], C. Klein-Bösing [137], M. Kleiner [64], T. Klemenz [95], A. Kluge [33], A.G. Knospe [115], C. Kobdaj [105], T. Kollegger[97], A. Kondratyev [143], N. Kondratyeva [142], E. Kondratyuk [142], J. Konig [64], S.A. Konigstorfer [95], P.J. Konopka [33], G. Kornakov [135], M. Korwieser [95], S.D. Koryciak [2], A. Kotliarov [86], V. Kovalenko [142], M. Kowalski [107], V. Kozhuharov [37], I. Králik [60], A. Kravčáková [38], L. Krcal [33,39], M. Krivda [100,60], F. Krizek [86], K. Krizkova Gajdosova [33], M. Kroesen [94], M. Krüger [64], D.M. Krupova [36], E. Kryshen [142], V. Kučera [58], C. Kuhn [128], P.G. Kuijer [84], T. Kumaoka[124], D. Kumar[134], L. Kumar [90], N. Kumar[90], S. Kumar [32], S. Kundu [33], P. Kurashvili [79], A. Kurepin [142], A.B. Kurepin [142], A. Kuryakin [142], S. Kushpil [86], V. Kuskov[142], M.J. Kweon [58], Y. Kwon [140], S.L. La Pointe [39], P. La Rocca [27], A. Lakrathok[105], M. Lamanna [33], R. Langoy [120], P. Larionov [33], E. Laudi [33], L. Lautner [33,95], R. Lavicka [102], R. Lea [133,55], H. Lee [104], I. Legrand [46], G. Legras [137], J. Lehrbach [39], T.M. Lelek[2], R.C. Lemmon [85], I. León Monzón [109], M.M. Lesch [95], E.D. Lesser [19], P. Lévai [138], X. Li[10], J. Lien [120], R. Lietava [100], I. Likmeta [115], B. Lim [25], S.H. Lim [17], V. Lindenstruth [39], A. Lindner[46], C. Lippmann [97], D.H. Liu [6], J. Liu [118], G.S.S. Liveraro [111], I.M. Lofnes [21], C. Loizides [87], S. Lokos [107], J. Lomker [59], P. Loncar [34], X. Lopez [126], E. López Torres [7], P. Lu [97,119], F.V. Lugo [67], J.R. Luhder [137], M. Lunardon [28], G. Luparello [57], Y.G. Ma [40], M. Mager [33], A. Maire [128], M.V. Makariev [37], M. Malaev [142], G. Malfattore [26], N.M. Malik [91], Q.W. Malik[20], S.K. Malik [91], L. Malinina [VI,143], D. Mallick [130,80], N. Mallick [48], G. Mandaglio [31,53], S.K. Mandal [79], V. Manko [142], F. Manso [126], V. Manzari [50], Y. Mao [6], R.W. Marcjan [2], G.V. Margagliotti [24], A. Margotti [51], A. Marín [97], C. Markert [108], P. Martinengo [33], M.I. Martínez [45], G. Martínez García [103], M.P.P. Martins [110], S. Masciocchi [97], M. Masera [25], A. Masoni [52], L. Massacrier [130], O. Massen [59], A. Mastroserio [131,50], O. Matonoha [75], S. Mattiazzo [28], A. Matyja [107], C. Mayer [107], A.L. Mazuecos [33], F. Mazzaschi [25], M. Mazzilli [33], J.E. Mdhluli [122], Y. Melikyan [44], A. Menchaca-Rocha [67], J.E.M. Mendez [65], E. Meninno [102,29], A.S. Menon [115], M. Meres [13], S. Mhlanga[113,68], Y. Miake[124], L. Micheletti [33], D.L. Mihaylov [95], K. Mikhaylov [143,142], A.N. Mishra [138], D. Miśkowiec [97], A. Modak [4], B. Mohanty[80], M. Mohisin Khan[IV,16], M.A. Molander [44], S. Monira [135], C. Mordasini [116], D.A. Moreira De Godoy [137], I. Morozov [142], A. Morsch [33], T. Mrnjavac [33], V. Muccifora [49], S. Muhuri [134], J.D. Mulligan [74], A. Mulliri[23], M.G. Munhoz [110], R.H. Munzer [64], H. Murakami [123], S. Murray [113], L. Musa [33], J. Musinsky [60], J.W. Myrcha [135], B. Naik [122], A.I. Nambrath [19], B.K. Nandi [47], R. Nania [51], E. Nappi [50], A.F. Nassirpour [18], A. Nath [94], C. Nattrass [121], M.N. Naydenov [37], A. Neagu[20], A. Negru[125], E. Nekrasova[142], L. Nellen [65], R. Nepeivoda [75], S. Nese [20], G. Neskovic [39], N. Nicassio [50], B.S. Nielsen [83], E.G. Nielsen [83], S. Nikolaev [142], S. Nikulin [142], V. Nikulin [142], F. Noferini [51], S. Noh [12], P. Nomokonov [143], J. Norman [118], N. Novitzky [87], P. Nowakowski [135], A. Nyanin [142], J. Nystrand [21], M. Ogino [76], S. Oh [18], A. Ohlson [75], V.A. Okorokov [142], J. Oleniacz [135], A.C. Oliveira Da Silva [121], A. Onnerstad [116], C. Oppedisano [56], A. Ortiz Velasquez [65], J. Otwinowski [107], M. Oya[92], K. Oyama [76], Y. Pachmayer [94], S. Padhan [47], D. Pagano [133,55], G. Paić [65], A. Palasciano [50], S. Panebianco [129],

H. Park [124], H. Park [104], J. Park [58], J.E. Parkkila [33], Y. Patley [47], R.N. Patra[91], B. Paul [23], H. Pei [6], T. Peitzmann [59], X. Peng [11], M. Pennisi [25], S. Perciballi [25], D. Peresunko [142], G.M. Perez [7], Y. Pestov[142], V. Petrov [142], M. Petrovici [46], R.P. Pezzi [103,66], S. Piano [57], M. Pikna [13], P. Pillot [103], O. Pinazza [51,33], L. Pinsky[115], C. Pinto [95], S. Pisano [49], M. Płoskoń [74], M. Planinic[89], F. Pliquett[64], M.G. Poghosyan [87], B. Polichtchouk [142], S. Politano [30], N. Poljak [89], A. Pop [46], S. Porteboeuf-Houssais [126], V. Pozdniakov [143], I.Y. Pozos [45], K.K. Pradhan [48], S.K. Prasad [4], S. Prasad [48], R. Preghenella [51], F. Prino [56], C.A. Pruneau [136], I. Pshenichnov [142], M. Puccio [33], S. Pucillo [25], Z. Pugelova[106], S. Qiu [84], L. Quaglia [25], S. Ragoni [15], A. Rai [139], A. Rakotozafindrabe [129], L. Ramello [132,56], F. Rami [128], S.A.R. Ramirez [45], T.A. Rancien[73], M. Rasa [27], S.S. Räsänen [44], R. Rath [51], M.P. Rauch [21], I. Ravasenga [84], K.F. Read [87,121], C. Reckziegel [112], A.R. Redelbach [39], K. Redlich [V,79], C.A. Reetz [97], A. Rehman[21], F. Reidt [33], H.A. Reme-Ness [35], Z. Rescakova[38], K. Reygers [94], A. Riabov [142], V. Riabov [142], R. Ricci [29], M. Richter [20], A.A. Riedel [95], W. Riegler [33], A.G. Riffero [25], C. Ristea [63], M.V. Rodriguez [33], M. Rodríguez Cahuantzi [45], K. Røed [20], R. Rogalev [142], E. Rogochaya [143], T.S. Rogoschinski [64], D. Rohr [33], D. Röhrich [21], P.F. Rojas[45], S. Rojas Torres [36], P.S. Rokita [135], G. Romanenko [26], F. Ronchetti [49], A. Rosano [31,53], E.D. Rosas[65], K. Roslon [135], A. Rossi [54], A. Roy [48], S. Roy [47], N. Rubini [26], D. Ruggiano [135], R. Rui [24], P.G. Russek [2], R. Russo [84], A. Rustamov [81], E. Ryabinkin [142], Y. Ryabov [142], A. Rybicki [107], H. Rytkonen [116], J. Ryu [17], W. Rzesa [135], O.A.M. Saarimaki [44], S. Sadhu [32], S. Sadovsky [142], J. Saetre [21], K. Šafařík [36], P. Saha[42], S.K. Saha [4], S. Saha [80], B. Sahoo [47], B. Sahoo [48], R. Sahoo [48], S. Sahoo[61], D. Sahu [48], P.K. Sahu [61], J. Saini [134], K. Sajdakova[38], S. Sakai [124], M.P. Salvan [97], S. Sambyal [91], D. Samitz [102], I. Sanna [33,95], T.B. Saramela[110], P. Sarma [42], V. Sarritzu [23], V.M. Sarti [95], M.H.P. Sas [33], S. Sawan[80], J. Schambach [87], H.S. Scheid [64], C. Schiaua [46], R. Schicker [94], F. Schlepper [94], A. Schmah[97], C. Schmidt [97], H.R. Schmidt[93], M.O. Schmidt [33], M. Schmidt[93], N.V. Schmidt [87], A.R. Schmier [121], R. Schotter [128], A. Schröter [39], J. Schukraft [33], K. Schweda [97], G. Scioli [26], E. Scomparin [56], J.E. Seger [15], Y. Sekiguchi[123], D. Sekihata [123], M. Selina [84], I. Selyuzhenkov [97], S. Senyukov [128], J.J. Seo [94,58], D. Serebryakov [142], L. Šerkšnytė [95], A. Sevcenco [63], T.J. Shaba [68], A. Shabetai [103], R. Shahoyan[33], A. Shangaraev [142], A. Sharma[90], B. Sharma [91], D. Sharma [47], H. Sharma [54], M. Sharma [91], S. Sharma [76], S. Sharma [91], U. Sharma [91], A. Shatat [130], O. Sheibani[115], K. Shigaki [92], M. Shimomura[77], J. Shin[12], S. Shirinkin [142], Q. Shou [40], Y. Sibiriak [142], S. Siddhanta [52], T. Siemiarczuk [79], T.F. Silva [110], D. Silvermyr [75], T. Simantathammakul[105], R. Simeonov [37], B. Singh[91], B. Singh [95], K. Singh [48], R. Singh [80], R. Singh [91], R. Singh [48], S. Singh [16], V.K. Singh [134], V. Singhal [134], T. Sinha [99], B. Sitar [13], M. Sitta [132,56], T.B. Skaali[20], G. Skorodumovs [94], M. Slupecki [44], N. Smirnov [139], R.J.M. Snellings [59], E.H. Solheim [20], J. Song [17], C. Sonnabend [33,97], F. Soramel [28], A.B. Soto-hernandez [88], R. Spijkers [84], I. Sputowska [107], J. Staa [75], J. Stachel [94], I. Stan [63], P.J. Steffanic [121], S.F. Stiefelmaier [94], D. Stocco [103], I. Storehaug [20], P. Stratmann [137], S. Strazzi [26], A. Sturniolo [31,53], C.P. Stylianidis[84], A.A.P. Suaide [110], C. Suire [130], M. Sukhanov [142], M. Suljic [33], R. Sultanov [142], V. Sumberia [91], S. Sumowidagdo [82], S. Swain[61], I. Szarka [13], M. Szymkowski [135], S.F. Taghavi [95], G. Taillepied [97], J. Takahashi [111], G.J. Tambave [80], S. Tang [6], Z. Tang [119], J.D. Tapia Takaki [117], N. Tapus[125], L.A. Tarasovicova [137], M.G. Tarzila [46], G.F. Tassielli [32], A. Tauro [33], G. Tejeda Muñoz [45], A. Telesca [33], L. Terlizzi [25], C. Terrevoli [115], S. Thakur [4], D. Thomas [108], A. Tikhonov [142], N. Tiltmann [33,137], A.R. Timmins [115], M. Tkacik[106], T. Tkacik [106], A. Toia [64], R. Tokumoto[92], K. Tomohiro[92], N. Topilskaya [142], M. Toppi [49], T. Tork [130], P.V. Torres[65], V.V. Torres [103], A.G. Torres Ramos [32], A. Trifiró [31,53], A.S. Triolo [33,31,53], S. Tripathy [51], T. Tripathy [47], S. Trogolo [33], V. Trubnikov [3], W.H. Trzaska [116], T.P. Trzcinski [135], A. Tumkin [142], R. Turrisi [54], T.S. Tveter [20], K. Ullaland [21], B. Ulukutlu [95], A. Uras [127], G.L. Usai [23], M. Vala[38], N. Valle [22], L.V.R. van Doremalen[59], M. van Leeuwen [84], C.A. van Veen [94], R.J.G. van Weelden [84], P. Vande Vyvre [33], D. Varga [138], Z. Varga [138], M. Vasileiou [78], A. Vasiliev [142], O. Vázquez Doce [49], O. Vazquez Rueda [115], V. Vechernin [142], E. Vercellin [25], S. Vergara Limón[45], R. Verma[47], L. Vermunt [97], R. Vértesi [138], M. Verweij [59], L. Vickovic[34], Z. Vilakazi[122], O. Villalobos Baillie [100], A. Villani [24], A. Vinogradov [142], T. Virgili [29], M.M.O. Virta [116], V. Vislavicius[75], A. Vodopyanov [143], B. Volkel [33], M.A. Völkl [94], K. Voloshin[142], S.A. Voloshin [136], G. Volpe [32], B. von Haller [33], I. Vorobyev [95], N. Vozniuk [142], J. Vrláková [38], J. Wan[40], C. Wang [40], D. Wang[40], Y. Wang [40], Y. Wang [6], A. Wegrzynek [33], F.T. Weiglhofer[39], S.C. Wenzel [33], J.P. Wessels [137], S.L. Weyhmiller [139], J. Wiechula [64], J. Wikne [20], G. Wilk [79], J. Wilkinson [97], G.A. Willems [137], B. Windelband [94], M. Winn [129], J.R. Wright [108], W. Wu[40], Y. Wu [119], R. Xu [6], A. Yadav [43], A.K. Yadav [134],

S. Yalcin [72], Y. Yamaguchi [92], S. Yang[21], S. Yano [92], E.R. Yeats[19], Z. Yin [6], I.-K. Yoo [17], J.H. Yoon [58], H. Yu[12], S. Yuan[21], A. Yuncu [94], V. Zaccolo [24], C. Zampolli [33], F. Zanone [94], N. Zardoshti [33], A. Zarochentsev [142], P. Závada [62], N. Zaviyalov[142], M. Zhalov [142], B. Zhang [6], C. Zhang [129], L. Zhang [40], S. Zhang [40], X. Zhang [6], Y. Zhang[119], Z. Zhang [6], M. Zhao [10], V. Zherebchevskii [142], Y. Zhi[10], D. Zhou [6], Y. Zhou [83], J. Zhu [54,6], Y. Zhu[6], S.C. Zugravel [56], N. Zurlo [133,55]

Affiliation Notes

[I] Also at: Max-Planck-Institut für Physik, Munich, Germany
[II] Also at: Italian National Agency for New Technologies, Energy and Sustainable Economic Development (ENEA), Bologna, Italy
[III] Also at: Dipartimento DET del Politecnico di Torino, Turin, Italy
[IV] Also at: Department of Applied Physics, Aligarh Muslim University, Aligarh, India
[V] Also at: Institute of Theoretical Physics, University of Wroclaw, Poland
[VI] Also at: An institution covered by a cooperation agreement with CERN

Collaboration Institutes

[1] A.I. Alikhanyan National Science Laboratory (Yerevan Physics Institute) Foundation, Yerevan, Armenia
[2] AGH University of Krakow, Cracow, Poland
[3] Bogolyubov Institute for Theoretical Physics, National Academy of Sciences of Ukraine, Kiev, Ukraine
[4] Bose Institute, Department of Physics and Centre for Astroparticle Physics and Space Science (CAPSS), Kolkata, India
[5] California Polytechnic State University, San Luis Obispo, California, United States
[6] Central China Normal University, Wuhan, China
[7] Centro de Aplicaciones Tecnológicas y Desarrollo Nuclear (CEADEN), Havana, Cuba
[8] Centro de Investigación y de Estudios Avanzados (CINVESTAV), Mexico City and Mérida, Mexico
[9] Chicago State University, Chicago, Illinois, United States
[10] China Institute of Atomic Energy, Beijing, China
[11] China University of Geosciences, Wuhan, China
[12] Chungbuk National University, Cheongju, Republic of Korea
[13] Comenius University Bratislava, Faculty of Mathematics, Physics and Informatics, Bratislava, Slovak Republic
[14] COMSATS University Islamabad, Islamabad, Pakistan
[15] Creighton University, Omaha, Nebraska, United States
[16] Department of Physics, Aligarh Muslim University, Aligarh, India
[17] Department of Physics, Pusan National University, Pusan, Republic of Korea
[18] Department of Physics, Sejong University, Seoul, Republic of Korea
[19] Department of Physics, University of California, Berkeley, California, United States
[20] Department of Physics, University of Oslo, Oslo, Norway
[21] Department of Physics and Technology, University of Bergen, Bergen, Norway
[22] Dipartimento di Fisica, Università di Pavia, Pavia, Italy
[23] Dipartimento di Fisica dell'Università and Sezione INFN, Cagliari, Italy
[24] Dipartimento di Fisica dell'Università and Sezione INFN, Trieste, Italy
[25] Dipartimento di Fisica dell'Università and Sezione INFN, Turin, Italy
[26] Dipartimento di Fisica e Astronomia dell'Università and Sezione INFN, Bologna, Italy
[27] Dipartimento di Fisica e Astronomia dell'Università and Sezione INFN, Catania, Italy
[28] Dipartimento di Fisica e Astronomia dell'Università and Sezione INFN, Padova, Italy
[29] Dipartimento di Fisica 'E.R. Caianiello' dell'Università and Gruppo Collegato INFN, Salerno, Italy
[30] Dipartimento DISAT del Politecnico and Sezione INFN, Turin, Italy
[31] Dipartimento di Scienze MIFT, Università di Messina, Messina, Italy
[32] Dipartimento Interateneo di Fisica 'M. Merlin' and Sezione INFN, Bari, Italy
[33] European Organization for Nuclear Research (CERN), Geneva, Switzerland
[34] Faculty of Electrical Engineering, Mechanical Engineering and Naval Architecture, University of Split, Split, Croatia
[35] Faculty of Engineering and Science, Western Norway University of Applied Sciences, Bergen, Norway

[36] Faculty of Nuclear Sciences and Physical Engineering, Czech Technical University in Prague, Prague, Czech Republic
[37] Faculty of Physics, Sofia University, Sofia, Bulgaria
[38] Faculty of Science, P.J. Šafárik University, Košice, Slovak Republic
[39] Frankfurt Institute for Advanced Studies, Johann Wolfgang Goethe-Universität Frankfurt, Frankfurt, Germany
[40] Fudan University, Shanghai, China
[41] Gangneung-Wonju National University, Gangneung, Republic of Korea
[42] Gauhati University, Department of Physics, Guwahati, India
[43] Helmholtz-Institut für Strahlen- und Kernphysik, Rheinische Friedrich-Wilhelms-Universität Bonn, Bonn, Germany
[44] Helsinki Institute of Physics (HIP), Helsinki, Finland
[45] High Energy Physics Group, Universidad Autónoma de Puebla, Puebla, Mexico
[46] Horia Hulubei National Institute of Physics and Nuclear Engineering, Bucharest, Romania
[47] Indian Institute of Technology Bombay (IIT), Mumbai, India
[48] Indian Institute of Technology Indore, Indore, India
[49] INFN, Laboratori Nazionali di Frascati, Frascati, Italy
[50] INFN, Sezione di Bari, Bari, Italy
[51] INFN, Sezione di Bologna, Bologna, Italy
[52] INFN, Sezione di Cagliari, Cagliari, Italy
[53] INFN, Sezione di Catania, Catania, Italy
[54] INFN, Sezione di Padova, Padova, Italy
[55] INFN, Sezione di Pavia, Pavia, Italy
[56] INFN, Sezione di Torino, Turin, Italy
[57] INFN, Sezione di Trieste, Trieste, Italy
[58] Inha University, Incheon, Republic of Korea
[59] Institute for Gravitational and Subatomic Physics (GRASP), Utrecht University/Nikhef, Utrecht, Netherlands
[60] Institute of Experimental Physics, Slovak Academy of Sciences, Košice, Slovak Republic
[61] Institute of Physics, Homi Bhabha National Institute, Bhubaneswar, India
[62] Institute of Physics of the Czech Academy of Sciences, Prague, Czech Republic
[63] Institute of Space Science (ISS), Bucharest, Romania
[64] Institut für Kernphysik, Johann Wolfgang Goethe-Universität Frankfurt, Frankfurt, Germany
[65] Instituto de Ciencias Nucleares, Universidad Nacional Autónoma de México, Mexico City, Mexico
[66] Instituto de Física, Universidade Federal do Rio Grande do Sul (UFRGS), Porto Alegre, Brazil
[67] Instituto de Física, Universidad Nacional Autónoma de México, Mexico City, Mexico
[68] iThemba LABS, National Research Foundation, Somerset West, South Africa
[69] Jeonbuk National University, Jeonju, Republic of Korea
[70] Johann-Wolfgang-Goethe Universität Frankfurt Institut für Informatik, Fachbereich Informatik und Mathematik, Frankfurt, Germany
[71] Korea Institute of Science and Technology Information, Daejeon, Republic of Korea
[72] KTO Karatay University, Konya, Turkey
[73] Laboratoire de Physique Subatomique et de Cosmologie, Université Grenoble-Alpes, CNRS-IN2P3, Grenoble, France
[74] Lawrence Berkeley National Laboratory, Berkeley, California, United States
[75] Lund University Department of Physics, Division of Particle Physics, Lund, Sweden
[76] Nagasaki Institute of Applied Science, Nagasaki, Japan
[77] Nara Women's University (NWU), Nara, Japan
[78] National and Kapodistrian University of Athens, School of Science, Department of Physics , Athens, Greece
[79] National Centre for Nuclear Research, Warsaw, Poland
[80] National Institute of Science Education and Research, Homi Bhabha National Institute, Jatni, India
[81] National Nuclear Research Center, Baku, Azerbaijan
[82] National Research and Innovation Agency - BRIN, Jakarta, Indonesia
[83] Niels Bohr Institute, University of Copenhagen, Copenhagen, Denmark
[84] Nikhef, National institute for subatomic physics, Amsterdam, Netherlands
[85] Nuclear Physics Group, STFC Daresbury Laboratory, Daresbury, United Kingdom
[86] Nuclear Physics Institute of the Czech Academy of Sciences, Husinec-Řež, Czech Republic
[87] Oak Ridge National Laboratory, Oak Ridge, Tennessee, United States

[88] Ohio State University, Columbus, Ohio, United States
[89] Physics department, Faculty of science, University of Zagreb, Zagreb, Croatia
[90] Physics Department, Panjab University, Chandigarh, India
[91] Physics Department, University of Jammu, Jammu, India
[92] Physics Program and International Institute for Sustainability with Knotted Chiral Meta Matter (SKCM2), Hiroshima University, Hiroshima, Japan
[93] Physikalisches Institut, Eberhard-Karls-Universität Tübingen, Tübingen, Germany
[94] Physikalisches Institut, Ruprecht-Karls-Universität Heidelberg, Heidelberg, Germany
[95] Physik Department, Technische Universität München, Munich, Germany
[96] Politecnico di Bari and Sezione INFN, Bari, Italy
[97] Research Division and ExtreMe Matter Institute EMMI, GSI Helmholtzzentrum für Schwerionenforschung GmbH, Darmstadt, Germany
[98] Saga University, Saga, Japan
[99] Saha Institute of Nuclear Physics, Homi Bhabha National Institute, Kolkata, India
[100] School of Physics and Astronomy, University of Birmingham, Birmingham, United Kingdom
[101] Sección Física, Departamento de Ciencias, Pontificia Universidad Católica del Perú, Lima, Peru
[102] Stefan Meyer Institut für Subatomare Physik (SMI), Vienna, Austria
[103] SUBATECH, IMT Atlantique, Nantes Université, CNRS-IN2P3, Nantes, France
[104] Sungkyunkwan University, Suwon City, Republic of Korea
[105] Suranaree University of Technology, Nakhon Ratchasima, Thailand
[106] Technical University of Košice, Košice, Slovak Republic
[107] The Henryk Niewodniczanski Institute of Nuclear Physics, Polish Academy of Sciences, Cracow, Poland
[108] The University of Texas at Austin, Austin, Texas, United States
[109] Universidad Autónoma de Sinaloa, Culiacán, Mexico
[110] Universidade de São Paulo (USP), São Paulo, Brazil
[111] Universidade Estadual de Campinas (UNICAMP), Campinas, Brazil
[112] Universidade Federal do ABC, Santo Andre, Brazil
[113] University of Cape Town, Cape Town, South Africa
[114] University of Derby, Derby, United Kingdom
[115] University of Houston, Houston, Texas, United States
[116] University of Jyväskylä, Jyväskylä, Finland
[117] University of Kansas, Lawrence, Kansas, United States
[118] University of Liverpool, Liverpool, United Kingdom
[119] University of Science and Technology of China, Hefei, China
[120] University of South-Eastern Norway, Kongsberg, Norway
[121] University of Tennessee, Knoxville, Tennessee, United States
[122] University of the Witwatersrand, Johannesburg, South Africa
[123] University of Tokyo, Tokyo, Japan
[124] University of Tsukuba, Tsukuba, Japan
[125] University Politehnica of Bucharest, Bucharest, Romania
[126] Université Clermont Auvergne, CNRS/IN2P3, LPC, Clermont-Ferrand, France
[127] Université de Lyon, CNRS/IN2P3, Institut de Physique des 2 Infinis de Lyon, Lyon, France
[128] Université de Strasbourg, CNRS, IPHC UMR 7178, F-67000 Strasbourg, France, Strasbourg, France
[129] Université Paris-Saclay, Centre d'Etudes de Saclay (CEA), IRFU, Départment de Physique Nucléaire (DPhN), Saclay, France
[130] Université Paris-Saclay, CNRS/IN2P3, IJCLab, Orsay, France
[131] Università degli Studi di Foggia, Foggia, Italy
[132] Università del Piemonte Orientale, Vercelli, Italy
[133] Università di Brescia, Brescia, Italy
[134] Variable Energy Cyclotron Centre, Homi Bhabha National Institute, Kolkata, India
[135] Warsaw University of Technology, Warsaw, Poland
[136] Wayne State University, Detroit, Michigan, United States
[137] Westfälische Wilhelms-Universität Münster, Institut für Kernphysik, Münster, Germany
[138] Wigner Research Centre for Physics, Budapest, Hungary
[139] Yale University, New Haven, Connecticut, United States
[140] Yonsei University, Seoul, Republic of Korea

[141] Zentrum für Technologie und Transfer (ZTT), Worms, Germany
[142] Affiliated with an institute covered by a cooperation agreement with CERN
[143] Affiliated with an international laboratory covered by a cooperation agreement with CERN.